nitrosative stess (arginine, paraquat and SIN-1) or oxidative stress (rotenone, 3-NP, sodium azide, MPP+, sodium arsenite and paraquat) were prepared in dH_2O and added at indicated concentrations and the medium was briefly mixed by aspiration. Incubations were performed for periods stated in individual experiments. Where indicated, cells were co-treated with kinase inhibitors (SP600125 (JNK), BI-78D3 (JNK), PD98095 & U0126 (ERK), SB203580 & SB202190 (p38), D4476 (casein kinase 1) from stock solutions prepared at 10 mM in DMSO. Control cultures were treated with vehicle alone. For immunoblotting, cells were harvested into Phosphosafe Extraction Buffer (Merck Biosciences, San Diego, CA, USA) containing protease inhibitor cocktail (Roche Diagnostics) and stored at -80°C until use. For immunofluorescence studies, cells were grown on glass coverslips and fixed by treating with 4% paraformaldehyde for 30 min.

siRNA knockdown of JNK

ON-TARGETPlus human JNK1 siRNA pool, JNK2 siRNA pool and non-targeting siRNA pool (D-001810-10-20, Negative control) were obtained from Dharmacon and resuspended in RNAase free water at 100 μM. Human JNK1 siRNA pool target sequences were 5'-GCCCAGUAAUAUAGUAGUA-3', 5'-GGCAUGGGCUACAAGGAAA-3', 5'-GAAUAGUAUGCGCAGCUUA-3' and 5'-GAUGACGCCUUAUGUAGUG-3'. Human JNK2 siRNA pool target sequences were 5'-UCGUGAACUUGUCCUCUUA-3', 5'-AGCCAACUGUGAGGAAUUA-3', 5'-GGCUGUCGAUGAUAGGUUA-3' and 5'-GAUUGUUUGUGCUGCAUUU-3'. Cells were seeded on coverslips at 5×10^4 cells per cm^2 in Opti-MeM to give 40% confluency on treatment day. Cells were transfected with pooled JNK1 and JNK2 siRNA or Negative control siRNA in Lipfectamine 2000 for 5 hr at room temperature (0.5 μg RNA per well). Media was then replaced with normal SY5Y growth medium overnight before treatment with paraquat (1 mM) overnight. Cells were then collected for Western blot for JNK or fixed for immunofluoresence of TDP-43 and HuR.

Western blot analysis of protein expression and phosphorylation

Cell lysates prepared in Phosphosafe Extraction Buffer at equal protein concentration were mixed with electrophoresis SDS sample buffer and separated on 12% SDS-PAGE Tris-Glycine gels. Proteins were transferred to PVDF membranes and blocked with 4% skim milk solution in PBST before immunoblotting for total or phospho-specific proteins. For detection of total TDP-43, membranes were probed with polyclonal antisera (1:1500) against TDP-43. Secondary antiserum was rabbit-HRP at 1:5,000 dilution. For detection of total and phospho-forms of JNK, ERK and p38, membranes were probed with anti-JNK, anti-ERK or anti-p38 (each at 1:5000) and antisera to phospho-forms of each protein (each at 1:5000). Blots were developed using GE Healthcare ECL Advance Chemiluminescence and imaged on a Fujifilm LAS3000 imager (Berthold, Bundoora, Australia). Expression of GAPDH or actin was determined using antisera at 1:5000 and 1:3000 respectively for protein loading controls where necessary.

Immunofluorescence analysis

SH-SY5Y cells were grown on 12 mm diameter coverslips and treated with stresses as indicated. Cells were fixed with 4% w/v paraformaldehyde in PBS for 30 min and permeabilized with 90% chilled methanol for 5 min. After blocking for 1 hr with 10% normal goat serum, cells were incubated with primary antibody for total TDP-43 (1:1500), ubiquitin (1:150), HuR (1:50), hnRNP A1 (1:200) or hnRNP K (1:200) for 2 hr at room temperature or overnight at 4°C. This was followed by labeling with secondary AlexaFluor or FITC goat anti-mouse or anti-rabbit antisera at 1:500 for 2 hr at room temperature or overnight at 4°C. After washing, the coverslips were incubated with DAPI at 0.5 μg/ml for 5 min and analyzed using a Leica inverted microscope with Zeiss Axiocam digital camera. Images shown are representative of multiple fields and triplicate coverslips per experiment. TDP-43 and HuR-positive stress granules (SGs) were counted in cultures where indicated. A minimum of 500 cells was counted across multiple fields of view (and multiple coverslips) for each treatment. The number of TDP-43 and HuR-positive SGs were counted in these cells. The total number of cells was divided by the total number of SGs to provide a measure of mean SGs per cell. SGs were not observed in untreated cells.

Preparation of TDP-43 plasmids

Plasmid DNA corresponding to GFP-tagged full-length wild-type (WT) TDP-43 (pEGFP-TDP WT), C-terminal fragments of TDP-43, (pEGFP-TDP 162-414 and pEGFP-TDP 219-414) or empty expression vector pEGFP-C1 were prepared as described by Nonaka et al. [15]. Briefly, plasmid DNA was used to transform MAX Efficiency® DH5α™ Competent Cells (Invitrogen, Mount Waverley, Victoria, Australia) as described by the manufacturer. Transformants were grown and colonies were picked based on kanamycin-resistance and grown in liquid culture for subsequent plasmid purification. DNA was purified using the Wizard® *Plus* Midiprep DNA Purification System (Promega Corporation) as per manufacturer's instructions. DNA was quantified and TDP-43 inserts were identified positively by digestion with *BamHI* and *XhoI*.

Transfection and expression of plasmids

SH-SY5Y cells were seeded at 2×10^5 cells per well in 24 well-plates on coverslips. Cells were transfected 24 hr after seeding with the pEGFP-C1 empty vector, pEGFP-TDP WT, pEGFP-TDP 162-414 and pEGFP-TDP 219-414 using Attractene (Qiagen) according to manufacturer's instructions. After 48 hr incubation, cells were fixed with 4% w/v paraformaldehyde in PBS for 30 min. and permeabilized with 90% chilled methanol for 5 min. After washing, the coverslips were incubated with DAPI at 0.5 μg/ml for 5 min and analyzed using a Leica inverted microscope with Zeiss Axiocam digital camera. Expression of TDP-43 was determined by the EGFP-tagged construct. Efficiency of transfection with pEGFP-C1 vector was approximately 20-25%.

Statistical analysis

All data described in graphical representations are mean ± standard error of the mean (SEM) unless stated from a minimum of three experiments. Results were analysed using a two-tailed Student's *t*-test.

Additional material

Additional file 1: SH-SY5Y cell viability after exposure to nitrosative or oxidative stress inducers. SH-SY5Y cells were treated with indicated compounds overnight and cell viability was measured with the MTT assay. **A:** Mild neurotoxicity was induced with all compounds tested. Concentrations were SIN-1, 0.1 mM; arginine, 1 mM; Paraquat, 1 mM and 2 mM; 3-NP, 1 mM; MPP+, 2 mM; sodium azide, 5 mM and rotenone, 0.075 mM. **B:** Comparison of neurotoxicity induced by 1 and 2 mM paraquat or 0.05 mM and 0.5 mM arsenite treatment overnight. *p < 0.05, **p < 0.01. n = three experiments.

Additional file 2: Treatment of SH-SY5Y neurons induces SG formation associated with mild toxicity. Non-differentiated (**A-C**) or differentiated (**D-K**) were treated with 0-2 mM (**A-C**) or 1 mM (**D-K**) paraquat overnight. **A**: Cell viability was determined by MTT assay. **B**: Cell death was determined by LDH assay. **C**: Stress granules (SGs) per cell were determined. *p < 0.05, **p < 0.01. **D-K**: TDP-43 and HuR immunofluorescence was examined in retinoic acid-differentiated neurons after treatment with 1 mM paraquat. Green = TDP-43, Red = HuR, Blue = DAPI. Arrows indicate SGs. Bar = 10 μm. **G** and **K** represent merged images. n = three experiments.

Additional file 3: Paraquat treatment did not induce phosphorylation of TDP-43 in SGs. Cells were treated overnight with 1 mM paraquat and examined for phosphorylated TDP-43 by immunofluorescence. **A-C:** untreated, **D-F:** paraquat treated. Green = HuR, Red = phospho-TDP-43, blue = DAPI. Bar = 10 μm. **G:** Immunoblot for phospho-TDP-43 (p-TDP-43) in paraquat-treated cultures. Representative images from three separate experiments.

Additional file 4: Treatment of SH-SY5Y cells with different mitochondrial inhibitors did not induce HuR SGs. Cells were treated with vehicle control (**A-B**), 2 mM MPP+ (**C-D**), 1 mM 3-NP (**E-F**), 0.075 mM rotenone (**G-H**) or 5 mM sodium azide (**I-J**). Cells were analyzed for HuR localization by immunofluorescence. Red = HuR, blue = DAPI. Bar = 10 μm. **K:** Treatment with 1 mM paraquat (PQ) overnight induced phospho-JNK (pJNK) and this was inhibited by co-treatment with 20 μM SP600125. Representative images from three separate experiments.

Additional file 5: Treatment of SH-SY5Y cells with siRNA to JNK inhibits TDP-43 accumulation in SGs. A: Cells were treated with pooled siRNA against JNK1 and JNK2 or with negative control siRNA and examined for JNK expression. siRNA to JNK significantly reduced expression of JNK1 and JNK2. **B-E:** Untreated control cells. **F-I:** cells treated with negative control siRNA reveal TDP-43 and HuR-positive SGs. **J-M:** Cells treated with siRNA to JNK reveal lack of TDP-43 but not HuR-positive SGs. Green = TDP-43, red = HuR, blue - DAPI. Arrows indicate SGs. Bar = 10 μm. Representative images from two-three separate experiments performed in triplicate.

Additional file 6: Treatment of U87MG astroglial and HeLa epithelial cells with paraquat results in TDP-43 SGs. U87MG (**A-F**) and HeLa (**G-L**) cells were treated overnight with 1 mM paraquat and analyzed for TDP-43 and HuR localization by immunofluorescence. **A-C**: Untreated U87MG cells, **D-F**: paraquat-treated U87MG cells, **G-I**: untreated HeLa cells, **J-L**: paraquat-treated HeLa cells. Green = TDP-43, red = HuR, blue = DAPI. Arrows indicate SGs. Bar = 10 μm. Representative images from three separate experiments performed in duplicate or triplicate.

Abbreviations

ALS: amyotrophic lateral sclerosis; CTF: C-terminal fragment; ERK: extracellular signal-regulated kinase; FTD: frontotemporal dementia; hnRNP: heterogeneous nuclear ribonucleoprotein; JNK: c-JUN N-terminal kinase; SG: stress granule; SOD: superoxide dismutase; TDP-43: TARDP-binding protein 43.

Acknowledgements

This work was supported by funding from the National Health and Medical Research Council of Australia (program grant to ARW and CLM) and the Australian Research Council of Australia (ARC Future Fellowship to Anthony White). Dominic Ng is a recipient of a Faculty of Medicine, Dentistry and Health Sciences, CR Roper Fellowship. Peter Crouch is recipient of a Melbourne Neuroscience Institute Research Fellowship. We would also like to thank the Motor Neuron Disease Research Institute of Australia (Mick Rodger Benalla Research Grant), the Bethlehem Griffiths Research Foundation and the CASS Foundation for their kind support of this work. JM was supported by Motor Neuron Disease Research Institute of Australia (Mick Rodger Benalla Research Grant). SJP was supported by the CASS foundation. LJV was supported by the NHMRC. KAP was supported by The University of Melbourne. JRL, AC, Q-XL and PJC were supported by the NHMRC. KMK was supported by Sigrid Juselius Foundation, Finland. CLM was supported by the Mental Health Research Institute. TN and HM were supported by the Tokyo Institute of Psychiatry.

Author details

[1]Department of Pathology, The University of Melbourne, Victoria, 3010, Australia. [2]Ludwig Institute for Cancer Research, Austin Hospital, Harold Stokes Building, 145-163 Studley Road, Heidelberg, Victoria, 3084, Australia. [3]Bio21 Molecular Science and Biotechnology Institute, The University of Melbourne, Parkville, Victoria, 3052, Australia. [4]Department of Biochemistry and Molecular Biology, The University of Melbourne, Parkville, Victoria, 3052, Australia. [5]The Mental Health Research Institute, Parkville, Victoria, 3052, Australia. [6]Department of Molecular Neurobiology, Tokyo Institute of Psychiatry, Tokyo 156-8585, Japan.

Authors' contributions

JM performed cell culture assays, immunofluorescence studies, immunoblotting and contributed to the preparation of the manuscript. SJP performed cell culture assays, immunofluorescence studies, immunoblotting transfected cells with constructs and contributed to the preparation of the manuscript. LJV prepared TDP-43 CTF constructs. KAP prepared, treated and collected cell cultures for analysis. JRL participated in the study design and coordination, contributed to experimental data collection and helped to draft the manuscript. AC performed cell culture assays, immunofluorescence studies, immunoblotting and contributed to the preparation of the manuscript, Q-XL participated in the study design and coordination, contributed to experimental data collection and helped to draft the manuscript. CLM helped to draft the manuscript. TN generated TDP-43 constructs. MH generated TDP-43 constructs. KMK participated in the study design and coordination, contributed to experimental data collection and helped to draft the manuscript. DCHN and MAB developed molecular tools

for JNK analysis and contributed to the preparation of the manuscript. PJC participated in the study design and coordination, contributed to experimental data collection and helped to draft the manuscript. ARW conceived the study, participated in the study design and coordination, and helped to draft the manuscript. All authors read and approved the final manuscript.

Competing interests

The authors declare that they have no competing interests.

Received: 15 April 2011 Accepted: 8 August 2011
Published: 8 August 2011

References

1. King AE, Dickson TC, Blizzard CA, Woodhouse A, Foster SS, Chung RS, Vickers JC: **Neuron-glia interactions underlie ALS-like axonal cytoskeletal pathology.** *Neurobiol Aging* 2009, **32**:459-469.
2. Barber SC, Shaw PJ: **Oxidative stress in ALS: key role in motor neuron injury and therapeutic target.** *Free Radic Biol Med* 2010, **48**:629-641.
3. Swarup V, Julien JP: **ALS pathogenesis: Recent insights from genetics and mouse models.** *Prog Neuropsychopharmacol Biol Psychiatry* 2010, **35**:363-369.
4. Barmada SJ, Finkbeiner S: **Pathogenic TARDBP mutations in amyotrophic lateral sclerosis and frontotemporal dementia: disease-associated pathways.** *Rev Neurosci* 2010, **21**:251-272.
5. Ferrari R, Kapogiannis D, Huey ED, Momeni P: **FTD and ALS: A Tale of Two Diseases.** *Curr Alzheimer Res* 2011, **8**:273-294.
6. Neumann M, Sampathu DM, Kwong LK, Truax AC, Micsenyi MC, Chou TT, Bruce J, Schuck T, Grossman M, Clark CM, McCluskey LF, Miller BL, Masliah E, Mackenzie IR, Feldman H, Feiden W, Kretzschmar HA, Trojanowski JQ, Lee VM: **Ubiquitinated TDP-43 in frontotemporal lobar degeneration and amyotrophic lateral sclerosis.** *Science* 2006, **314**:130-133.
7. Arai T, Hasegawa M, Akiyama H, Ikeda K, Nonaka T, Mori H, Mann D, Tsuchiya K, Yoshida M, Hashizume Y, Oda T: **TDP-43 is a component of ubiquitin-positive tau-negative inclusions in frontotemporal lobar degeneration and amyotrophic lateral sclerosis.** *Biochem Biophys Res Commun* 2006, **351**:602-611.
8. Chen-Plotkin AS, Lee VM, Trojanowski JQ: **TAR DNA-binding protein 43 in neurodegenerative disease.** *Nat Rev Neurol* 2010, **6**:211-220.
9. Banks GT, Kuta A, Isaacs AM, Fisher EM: **TDP-43 is a culprit in human neurodegeneration, and not just an innocent bystander.** *Mamm Genome* 2008, **19**:299-305.
10. Mackenzie IR, Rademakers R, Neumann M: **TDP-43 and FUS in amyotrophic lateral sclerosis and frontotemporal dementia.** *Lancet Neurol* 2010, **9**:995-1007.
11. Warraich ST, Yang S, Nicholson GA, Blair IP: **TDP-43: a DNA and RNA binding protein with roles in neurodegenerative diseases.** *Int J Biochem Cell Biol* 2010, **42**:1606-169.
12. Nishimura AL, Zupunski V, Troakes C, Kathe C, Fratta P, Howell M, Gallo JM, Hortobagyi T, Shaw CE, Rogelj B: **Nuclear import impairment causes cytoplasmic trans-activation response DNA-binding protein accumulation and is associated with frontotemporal lobar degeneration.** *Brain* 2010, **133**:1763-1771.
13. Igaz LM, Kwong LK, Chen-Plotkin A, Winton MJ, Unger TL, Xu Y, Neumann M, Trojanowski JQ, Lee VM: **Expression of TDP-43 C-terminal Fragments in Vitro Recapitulates Pathological Features of TDP-43 Proteinopathies.** *J Biol Chem* 2009, **284**:8516-24.
14. Zhang YJ, Xu YF, Cook C, Gendron TF, Roettges P, Link CD, Lin WL, Tong J, Castanedes-Casey M, Ash P, Gass J, Rangachari V, Buratti E, Baralle F, Golde TE, Dickson DW, Petrucelli L: **Aberrant cleavage of TDP-43 enhances aggregation and cellular toxicity.** *Proc Natl Acad Sci USA* 2009, **106**:7607-12.
15. Nonaka T, Kametani F, Arai T, Akiyama H, Hasegawa M: **Truncation and pathogenic mutations facilitate the formation of intracellular aggregates of TDP-43.** *Hum Mol Genet* 2009, **18**:3353-3364.
16. McDonald KK, Aulas A, Destroismaisons L, Pickles S, Beleac E, Camu W, Rouleau GA, Vande Velde C: **TAR DNA-binding protein 43 (TDP-43) regulates stress granule dynamics via differential regulation of G3BP and TIA-1.** *Hum Mol Genet* 2011, **20**:1400-1410.
17. Liu-Yesucevitz L, Bilgutay A, Zhang YJ, Vanderwyde T, Citro A, Mehta T, Zaarur N, McKee A, Bowser R, Sherman M, Petrucelli L, Wolozin B: **Tar DNA binding protein-43 (TDP-43) associates with stress granules: analysis of cultured cells and pathological brain tissue.** *PLoS One* 2010, **5**:e13250.
18. Buchan JR, Parker R: **Eukaryotic stress granules: the ins and outs of translation.** *Mol Cell* 2009, **36**:932-941.
19. Colombrita C, Zennaro E, Fallini C, Weber M, Sommacal A, Buratti E, Silani V, Ratti A: **TDP-43 is recruited to stress granules in conditions of oxidative insult.** *J Neurochem* 2009, **111**:1051-1061.
20. Dewey CM, Cenik B, Sephton CF, Dries DR, Mayer Pr, Good SK, Johnson BA, Herz J, Yu G: **TDP-43 is directed to stress granules by sorbitol, a novel physiological osmotic and oxidative stressor.** *Mol Cell Biol* 2010, **31**:1098-108.
21. Moisse K, Volkening K, Leystra-Lantz C, Welch I, Hill T, Strong MJ: **Divergent patterns of cytosolic TDP-43 and neuronal progranulin expression following axotomy: implications for TDP-43 in the physiological response to neuronal injury.** *Brain Res* 2009, **1249**:202-211.
22. Volkening K, Leystra-Lantz C, Yang W, Jaffee H, Strong MJ: **Tar DNA binding protein of 43 kDa (TDP-43), 14-3-3 proteins and copper/zinc superoxide dismutase (SOD1) interact to modulate NFL mRNA stability. Implications for altered RNA processing in amyotrophic lateral sclerosis (ALS).** *Brain Res* 2009, **1305**:168-182.
23. Ito D, Seki M, Tsunoda Y, Uchiyama H, Suzuki N: **Nuclear transport impairment of amyotrophic lateral sclerosis-linked mutations in FUS/TLS.** *Ann Neurol* 2011, **69**:152-162.
24. Dormann D, Rodde R, Edbauer D, Bentmann E, Fischer I, Hruscha A, Than ME, Mackenzie IR, Capell A, Schmid B, Neumann M, Haass C: **ALS-associated fused in sarcoma (FUS) mutations disrupt Transportin-mediated nuclear import.** *EMBO J* 2010, **29**:2841-2857.
25. Freibaum BD, Chitta RK, High AA, Taylor JP: **Global analysis of TDP-43 interacting proteins reveals strong association with RNA splicing and translation machinery.** *J Proteome Res* 2010, **9**:1104-1120.
26. Barber SC, Mead RJ, Shaw PJ: **Oxidative stress in ALS: A mechanism of neurodegeneration and a therapeutic target.** *Biochim Biophys Acta* 2006, **1762**:1051-1067.
27. Nonaka T, Arai T, Buratti E, Baralle FE, Akiyama H, Hasegawa M: **Phosphorylated and ubiquitinated TDP-43 pathological inclusions in ALS and FTLD-U are recapitulated in SH-SY5Y cells.** *FEBS Lett* 2009, **583**:394-400.
28. Caragounis A, Price KA, Soon CP, Filiz G, Masters CL, Li QX, Crouch PJ, White AR: **Zinc induces depletion and aggregation of endogenous TDP-43.** *Free Radic Biol Med* 2010, **48**:1152-1161.
29. Dormann D, Capell A, Carlson AM, Shankaran SS, Rodde R, Neumann M, Kremmer E, Matsuwaki T, Yamanouchi K, Nishihara M, Haass C: **Proteolytic processing of TAR DNA binding protein-43 by caspases produces C-terminal fragments with disease defining properties independent of progranulin.** *J Neurochem* 2009, **110**:1082-1094.
30. Nishimoto Y, Ito D, Yagi T, Nihei Y, Tsunoda Y, Suzuki N: **Characterization of alternative isoforms and inclusion body of the TAR DNA-binding protein-43.** *J Biol Chem* 2010, **285**:608-619.
31. Chang JW, Koike T, Iwashima M: **hnRNP-K is a nuclear target of TCR-activated ERK and required for T-cell late activation.** *Int Immunol* 2009, **21**:1351-1361.
32. Zhou R, Shanas R, Nelson MA, Bhattacharyya A, Shi J: **Increased expression of the heterogeneous nuclear ribonucleoprotein K in pancreatic cancer and its association with the mutant p53.** *Int J Cancer* 2010, **126**:395-404.
33. Buxade M, Parra JL, Rousseau S, Shpiro N, Marquez R, Morrice N, Bain J, Espel E, Proud CG: **The Mnks are novel components in the control of TNF alpha biosynthesis and phosphorylate and regulate hnRNP A1.** *Immunity* 2005, **23**:177-189.
34. Habelhah H, Shah K, Huang L, Ostareck-Lederer A, Burlingame AL, Shokat KM, Hentze MW, Ronai Z: **ERK phosphorylation drives cytoplasmic accumulation of hnRNP-K and inhibition of mRNA translation.** *Nat Cell Biol* 2001, **3**:325-330.
35. Shimada N, Rios I, Moran H, Sayers B, Hubbard K: **p38 MAP kinase-dependent regulation of the expression level and subcellular distribution of heterogeneous nuclear ribonucleoprotein A1 and its involvement in cellular senescence in normal human fibroblasts.** *RNA Biol* 2009, **6**:293-304.
36. Guil S, Long JC, Caceres JF: **hnRNP A1 relocalization to the stress granules reflects a role in the stress response.** *Mol Cell Biol* 2006, **26**:5744-5758.
37. Bogoyevitch MA, Ngoei KR, Zhao TT, Yeap YY, Ng DC: **c-Jun N-terminal kinase (JNK) signaling: recent advances and challenges.** *Biochim Biophys Acta* 2010, **1804**:463-745.

38. Yang W, Tiffany-Castiglioni E, Koh HC, Son IH: **Paraquat activates the IRE1/ASK1/JNK cascade associated with apoptosis in human neuroblastoma SH-SY5Y cells.** *Toxicol Lett* 2009, **191**:203-210.
39. Choi WS, Abel G, Klintworth H, Flavell RA, Xia Z: **JNK3 mediates paraquat- and rotenone-induced dopaminergic neuron death.** *J Neuropathol Exp Neurol* 2010, **69**:511-520.
40. Stebbins JL, De SK, Machleidt T, Becattini B, Vazquez J, Kuntzen C, Chen LH, Cellitti JF, Riel-Mehan M, Emdadi A, Solinas G, Karin M, Pellecchia M: **Identification of a new JNK inhibitor targeting the JNK-JIP interaction site.** *Proc Natl Acad Sci USA* 2008, **105**:16809-16813.
41. Wasserman T, Katsenelson K, Daniliuc S, Hasin T, Choder M, Aronheim A: **A novel c-Jun N-terminal kinase (JNK)-binding protein WDR62 is recruited to stress granules and mediates a nonclassical JNK activation.** *Mol Biol Cell* 2010, **21**:117-130.
42. Buratti E, Brindisi A, Giombi M, Tisminetzky S, Ayala YM, Baralle FE: **TDP-43 binds heterogeneous nuclear ribonucleoprotein A/B through its C-terminal tail: an important region for the inhibition of cystic fibrosis transmembrane conductance regulator exon 9 splicing.** *J Biol Chem* 2005, **280**:37572-37584.
43. Habelhah H, Shah K, Huang L, Burlingame AL, Shokat KM, Ronai Z: **Identification of new JNK substrate using ATP pocket mutant JNK and a corresponding ATP analogue.** *J Biol Chem* 2001, **276**:18090-18095.
44. Hostetter C, Licata LA, Witkiewicz A, Costantino CL, Yeo CJ, Brody JR, Keen JC: **Cytoplasmic accumulation of the RNA binding protein HuR is central to tamoxifen resistance in estrogen receptor positive breast cancer cells.** *Cancer Biol Ther* 2008, **7**:1496-1506.
45. D'Ambrogio A, Buratti E, Stuani C, Guarnaccia C, Romano M, Ayala YM, Baralle FE: **Functional mapping of the interaction between TDP-43 and hnRNP A2 in vivo.** *Nucleic Acids Res* 2009, **37**:4116-4126.
46. Perlson E, Jeong GB, Ross JL, Dixit R, Wallace KE, Kalb RG, Holzbaur EL: **A switch in retrograde signaling from survival to stress in rapid-onset neurodegeneration.** *J Neurosci* 2009, **29**:9903-9917.
47. Zhu X, Perry G, Smith MA: **Amyotrophic lateral sclerosis: a novel hypothesis involving a gained 'loss of function' in the JNK/SAPK pathway.** *Redox Rep* 2003, **8**:129-133.
48. Veglianese P, Lo Coco D, Bao Cutrona M, Magnoni R, Pennacchini D, Pozzi B, Gowing G, Julien JP, Tortarolo M, Bendotti C: **Activation of the p38MAPK cascade is associated with upregulation of TNF alpha receptors in the spinal motor neurons of mouse models of familial ALS.** *Mol Cell Neurosci* 2006, **31**:218-231.
49. Kim EK, Choi EJ: **Pathological roles of MAPK signaling pathways in human diseases.** *Biochim Biophys Acta* 2010, **1802**:396-405.
50. Atzori C, Ghetti B, Piva R, Srinivasan AN, Zolo P, Delisle MB, Mirra SS, Migheli A: **Activation of the JNK/p38 pathway occurs in diseases characterized by tau protein pathology and is related to tau phosphorylation but not to apoptosis.** *J Neuropathol Exp Neurol* 2001, **60**:1190-1197.
51. Ayala V, Granado-Serrano A, Cacabelos D, Naudí A, Ilieva V, Boada J, Caraballo-Miralles V, Lladó J, Ferrer I, Pamplona R, Portero-Otin M: **Cell stress induces TDP-43 pathological changes associated with ERK1/2 dysfunction: implications in ALS.** *Acta Neuropathol* 2011.
52. Migheli A, Piva R, Atzori C, Troost D, Schiffer D: **c-Jun, JNK/SAPK kinases and transcription factor NF-kappa B are selectively activated in astrocytes, but not motor neurons, in amyotrophic lateral sclerosis.** *J Neuropathol Exp Neurol* 1997, **56**:1314-1322.
53. Stevenson A, Yates DM, Manser C, De Vos KJ, Vagnoni A, Leigh PN, McLoughlin DM, Miller CC: **Riluzole protects against glutamate-induced slowing of neurofilament axonal transport.** *Neurosci Lett* 2009, **454**:161-164.

doi:10.1186/1750-1326-6-57
Cite this article as: Meyerowitz *et al.*: C-Jun N-terminal kinase controls TDP-43 accumulation in stress granules induced by oxidative stress. *Molecular Neurodegeneration* 2011 **6**:57.

The FASEB Journal • Research Communication

Phosphorylated α-synuclein can be detected in blood plasma and is potentially a useful biomarker for Parkinson's disease

Penelope G. Foulds,* J. Douglas Mitchell,‡ Angela Parker,‡ Roisin Turner,‡ Gerwyn Green,† Peter Diggle,† Masato Hasegawa,§ Mark Taylor,* David Mann,‖ and David Allsop*,[1]

*Division of Biomedical and Life Sciences and †Division of Health Research, School of Health and Medicine, University of Lancaster, Lancaster, UK; ‡Royal Preston Hospital, Preston, UK; §Department of Molecular Neurobiology, Tokyo Institute of Psychiatry, Tokyo, Japan; and ‖Neurodegeneration and Mental Health Research Group, School of Community-Based Medicine, University of Manchester, Hope Hospital, Salford, UK

ABSTRACT **Parkinson's disease (PD) is characterized by the presence of Lewy bodies containing phosphorylated and aggregated α-synuclein (α-syn). α-Syn is present in human body fluids, including blood plasma, and is a potential biomarker for PD. Immunoassays for total and oligomeric forms of both normal and phosphorylated (at Ser-129) α-syn have been used to assay plasma samples from a longitudinal cohort of 32 patients with PD (sampled at mo 0, 1, 2, 3), as well as single plasma samples from a group of 30 healthy control participants. The levels of α-syn in plasma varied greatly between individuals, but were remarkably consistent over time within the same individual with PD. The mean level of phospho-α-syn was found to be higher (P=0.053) in the PD samples than the controls, whereas this was not the case for total α-syn (P=0.244), oligo-α-syn (P=0.221), or oligo-phospho-α-syn (P=0.181). Immunoblots of plasma revealed bands (at 21, 24, and 50–60 kDa) corresponding to phosphorylated α-syn. Thus, phosphorylated α-syn can be detected in blood plasma and shows more promise as a diagnostic marker than the nonphosphorylated protein. Longitudinal studies undertaken over a more extended time period will be required to determine whether α-syn can act as a marker of disease progression.—Foulds, P. G., Mitchell, J. D., Parker, A., Turner, R., Green, G., Diggle, P., Hasegawa, M., Taylor, M., Mann, D., Allsop, D. Phosphorylated α-synuclein can be detected in blood plasma and is potentially a useful biomarker for Parkinson's disease. *FASEB J.* 25, 4127–4137 (2011). www.fasebj.org**

Key Words: Lewy body · oligomer · immunoassay · immunoblot

PARKINSON'S DISEASE (PD) is the second most common neurodegenerative disorder after Alzheimer's disease (AD) and is characterized clinically by the 3 cardinal motor symptoms of resting tremor, rigidity, and bradykinesia. Patients often exhibit further symptoms, including postural imbalance, gait disturbance, and a mask-like facial expression. In the advanced stages of PD, nonmotor symptoms can also appear, including anxiety, depression, dementia, and psychosis. The defining neuropathological features of idiopathic PD are the loss of dopaminergic neurons from the substantia nigra (SN) and the presence of Lewy bodies (LBs) and Lewy neurites (LNs) in surviving neurons of this and other brain regions (1). Similar lesions are present within the cerebral cortex in the related disorder of dementia with Lewy bodies (DLB; ref. 2). LBs and LNs contain a misfolded, fibrillar, and phosphorylated form of the protein α-synuclein (α-syn; refs. 1, 3). Pathological changes involving α-syn, chiefly in glial cells, also occur in multiple system atrophy (MSA), and, therefore, PD, DLB, and MSA are often collectively referred to as "α-syncleinopathies" (2). Duplication (4, 5), triplication (6), and mutation (7–9) of the gene encoding α-syn (*SNCA*) are all causes of hereditary forms of either PD or DLB. α-Syn oligomers are believed to be toxic to cells, as are oligomers derived from the various proteins associated with several other protein-misfolding neurodegenerative disorders, such as AD or the prion disorders (10, 11). Overexpression of wild-type or mutant α-syn in animal models can produce a phenotype resembling PD, including SN degeneration, movement problems and responsiveness to L-dopa therapy (12–15). Together, these observations suggest that α-syn plays a pivotal role in the development of the α-synucleinopathies (16).

PD is one of several neurological movement disor-

[1] Correspondence: Division of Biomedical and Life Sciences, School of Health and Medicine, University of Lancaster, Lancaster, LA1 4AY, UK. E-mail: d.allsop@lancaster.ac.uk

doi: 10.1096/fj.10-179192

This article includes supplemental data. Please visit *http://www.fasebj.org* to obtain this information.

ders that can produce similar symptoms, and a correct diagnosis is critically dependent on clinical examination to rule out disorders that can mimic PD. A diagnosis of PD is considered if the person exhibits more than one of the 3 cardinal motor symptoms mentioned above (17). The presence of resting tremor supports the diagnosis of PD more than the other two symptoms, but ~20% of patients with autopsy-confirmed PD fail to develop any resting tremor (18). Moreover, only 69–70% of people with autopsy-confirmed PD have at least two of the cardinal signs of the disease and 20–25% of people with two of these symptoms have a pathological diagnosis other than PD (19, 20). Perhaps even more surprising is the finding that 13–19% of people who demonstrate all three of the cardinal features have a pathological diagnosis other than PD (19, 20). Because the progression of neurological movement disorders and their treatment varies greatly, proper clinical diagnosis is essential for correct patient management. Furthermore, by the time PD is diagnosed, >60% of dopaminergic neurons in the SN can already be lost (21), making accurate early diagnosis, ideally before clinical symptoms appear, essential for any effective neuroprotective intervention strategy. Also, the clinical diagnosis of early PD may be difficult because although the patient might complain of symptoms suggesting PD, the neurological examination may be normal (22). These problems with clinical diagnosis have led to an increased interest in the development of diagnostic markers for PD, including advanced brain imaging methodologies (23) and molecular biomarkers (24). Genetic testing for mutations in genes linked to familial PD (including *SNCA*) is available (25), but it is only relevant when there is a strong family history, or when symptoms present at an unusually young age.

We have reported that α-syn is released from cells and is present in human body fluids, including cerebrospinal fluid (CSF) and blood plasma (26). This extracellular form of α-syn seems to be secreted from neuronal cells by exocytosis (27, 28) and could play an important role in cell-to-cell transfer of α-syn pathology in the brain (29). There is now an emerging consensus that the levels of α-syn are, on average, lower in samples of CSF taken from a group of patients with PD compared with a group of normal or neurological controls (30, 31), especially when the confounding variables of age and blood contamination are taken into account (32, 33). However, obtaining CSF is an invasive procedure, and analysis of α-syn levels in CSF is not generally amenable to longitudinal study. There are also some studies of α-syn as a potential biomarker in the much more accessible peripheral blood, with an initial report suggesting increased levels of this protein in plasma samples from patients with PD compared with those from healthy controls (34). However, subsequent studies have reported decreased levels of α-syn in PD plasma (35) or no significant change (36). We have shown that the levels of oligomeric α-syn appear to be significantly elevated in plasma samples from a group of patients with PD compared with a group of diseased controls (37). To develop this line of enquiry further, we have now set up a longitudinal study in newly diagnosed patients with PD to examine the levels of various different forms of α-syn, including phosphorylated and/or oligomeric forms, in blood plasma. Because α-syn accumulates in a phosphorylated and aggregated form in LBs (3), it is possible that these modified, pathological forms of the protein will more accurately reflect the fundamental neuropathology of PD than straightforward measures of "total" α-syn (33, 38). Our ultimate aim is to develop a relatively simple test for the early diagnosis of PD, or a surrogate marker for monitoring the progression of PD. Here, we report the results obtained during the initial phase of this longitudinal study.

MATERIALS AND METHODS

Patient population and clinical method

Participants for this study were recruited (with ethical approval, using appropriate consenting procedures) from the neurological service based at the Royal Preston Hospital along with other similar departments in the northwest of England. The diagnosis of PD was based on the UK Parkinson's Disease Society diagnostic criteria for PD (39). Severity of disease was defined in terms of patients satisfying the criteria for stages 1 or 2 on the Hoehn and Yahr scale.

The overall target for the study was to follow a cohort of 200 patients meeting these criteria over a period of 2–3 yr, reviewing them at 4- to 6-mo intervals. This study is ongoing, but the plan was also to follow the first 32 patients more intensively over the initial phases of the study, and this group was seen at monthly intervals for the first 3 mo. The results from these 32 patients over the first 3 mo are presented here. Blood samples were obtained from the participating sites (Preston and Arrowe Park). Around 3 ml of blood was collected in tubes containing EDTA, and the plasma was separated within 3 h by centrifuging the blood at 3000 *g* for 10 min. The plasma was immediately stored at −80°C. Appropriate care was taken to avoid contamination of the plasma samples with cells or components of the pellet obtained from the centrifugation. The samples were thawed at room temperature directly before analysis. Repeated freeze/thaw cycles were avoided.

Control subjects were healthy individuals with no apparent neurological or known psychiatric symptoms who were the spouses of patients attending the Cerebral Function Unit clinics at Hope Hospital (Salford Royal Hospital, National Health Service Foundation Trust) for investigation and diagnosis of dementia. These control subjects were recruited as part of an ongoing investigation into the genetics and molecular biology of dementia approved by the Oldham Local Research Ethics Committee. Blood plasma was prepared and stored as described above.

Preparation of recombinant α-syn

Recombinant α-syn (without any purification tag) was prepared at Lancaster University from *Escherichia coli* using the following protocol. pJEK2 was used to transform FB850, a *rec* A^- derivative of BL21 (DES) pLysS. FB850 carrying this plasmid was grown in an 800-ml batch culture, and protein expression was induced through the addition of isopropyl-β-

D-thiogalactopyranoside (IPTG). A protein with a molecular weight of ~17 kDa started to accumulate in the cells 30 min after induction and reached maximum levels after 150 min. Immunoblot analysis identified this protein as α-syn using an anti-α-syn mouse monoclonal antibody (MAb 211; Santa Cruz Biotechnology, Santa Cruz, CA, USA). After a 3-h induction, the suspension was centrifuged, and the cells were resuspended in buffer. The cells were lysed by sonication, and then cell debris and insoluble material were removed by centrifugation at 4°C for 1 h at 30,000 rpm. α-Syn was extracted from the supernatant by ammonium sulfate precipitation, then purified using two chromatography columns; mono Q and Superdex 200 (Amersham Biosciences, Piscataway, NJ, USA). After purification, 5 μg of protein ran as a single band when observed on a Coomassie blue-stained SDS gel, corresponding to monomeric α-syn.

Preparation of phosphorylated recombinant α-syn

Phosphorylated α-syn was prepared from recombinant α-syn, as described previously (40). Briefly, α-syn (630 μM) was incubated with casein kinase II (CK2; New England Biolabs, Ipswitch, MA, USA) in 1 ml of buffer containing 20 mM Tris-HCl (pH 7.5), 50 mM KCl, 10 mM $MgCl_2$, and 1 mM ATP at 30°C for 24 h. For effective phosphorylation, CK2 was added to the reaction mixture at 2-h intervals for the first 10 h (7500 U×5). The reaction was stopped by boiling for 5 min, cleared by centrifugation at 113,000 *g* for 20 min at 4°C, and then loaded onto a Resource Q anion-exchange column (Amersham Biosciences) equilibrated with 20 mM Tris-HCl (pH 8.0) and 0.2 M NaCl, and then eluted with a linear gradient of NaCl from 0.20 to 0.35 M for 15 min at a flow rate of 1 ml/min. Fractionated samples were analyzed by immunoblotting with a phosphorylation-dependent anti-α-syn antibody, PSer129 (Epitomics, Burlingame, CA, USA), and mass spectrometry. The PSer129-positive phosphorylated α-syn recovered in the fractions with ~0.3 M NaCl was concentrated by ammonium sulfate precipitation.

Preparation of oligomeric forms of recombinant α-syn

To prepare a standard for the oligomeric α-syn immunoassay, the recombinant protein was oligomerized by incubation at 45 μM in PBS in an orbital shaker at 37°C for 5 d, and the monomer and oligomer were separated by size-exclusion chromatography. A sample (0.5 ml) of preaggregated α-syn was loaded onto a Superdex 200 column (44×1 cm) connected to a fast protein liquid chromatography (FPLC) system (Atka Purifier; GE Healthcare, New York, NY, USA) and eluted with running buffer (PBS) at a flow rate of 0.5 ml/min. Absorbance of the eluate was monitored at 280 nm; fractions of 1 ml were collected, and protein concentration was determined.

To prepare a standard for the oligo-phospho-α-syn immunoassay, the phosphorylated protein was oligomerized by incubation at 50 μM in PBS in an orbital shaker at 37°C for 5 d. Aggregation of the protein was confirmed by thioflavin T assay. In this case, the amount of sample available was too small to fractionate by size-exclusion chromatography.

Immunoassay methods

We have already established immunoassay methods for the measurement of total and soluble oligomeric forms of α-syn in human biological fluids, including blood plasma (37, 41), and these methods have been further optimized.

Total α-syn

A 96-well microtiter plate (Iwaki, Holliston, MA, USA) was coated with 100 μl/well of anti-α-syn monoclonal antibody 211 diluted 1:1000 (0.2 μg/ml; Santa Cruz Biotechnology) in 50 mM $NaHCO_3$ (pH 9.6) and incubated at 4°C overnight. The wells were then washed 4 times with PBS containing 0.05% Tween-20 (PBS-T) and were incubated for 2 h at 37°C with 200 μl/well of freshly prepared blocking buffer (2.5% gelatin in PBS-T). The plate was washed again 4 times with PBS-T, and 100 μl of the assay standard or plasma samples was added to each well (each plasma sample was diluted 1:40 with PBS), and the assays were performed in triplicate. Following this, the plate was incubated at 37°C for 2 h. After a repeat washing with PBS-T, 100 μl/well of the detection antibody, anti-α/β/γ-synuclein FL-140 (Santa Cruz Biotechnology), dilution 1:750 (0.27 μg/ml) in blocking buffer was added, and the plate was incubated at 37°C for 2 h. After another wash with PBS-T, the plate was incubated with 100 μl/well of secondary antibody [goat anti-rabbit horseradish peroxidase (HRP); Sigma, St. Louis, MO, USA], dilution 1:10,000 in blocking buffer at 37°C for 2 h. The plate was then washed again with PBS-T before adding 100 μl/well of Sure Blue TMB microwell peroxidase substrate (KPL, Gaithersburg, MD, USA) and leaving the color to develop for 30 min at room temperature. Finally 100 μl/well of stop solution (0.3 M H_2SO_4) was added, and absorbance at 450 nm was determined. Recombinant monomeric α-syn was used to create a standard curve.

Oligomeric α-syn (oligo-α-syn)

The microtiter plate was coated and blocked using the same method as the assay for total α-syn. The wells were then washed 4 times with PBS-T, and 100 μl of the plasma sample (diluted 1:25 with PBS) or assay standard (oligo-α-syn) was added to each well, in triplicate. Following this, the plate was incubated at 37°C for 2 h. After a repeat wash with PBS-T, 100 μl/well of the detection antibody, biotinylated anti-α-synuclein 211 (diluted 1:1000 in blocking buffer) was added, and the plate was incubated at 37°C for 2 h. After another wash with PBS-T, the plate was incubated with 100 μl/well of streptavidin-europium, diluted 1:500 in streptavidin-europium buffer (Perkin Elmer, Wellesley, MA, USA) and shaken for 10 min. After a further 50-min agitation on a rotating platform, the plate was washed again with PBS-T, before adding 100 μl/well enhancer solution (Perkin Elmer). Finally, the plates were read on a Wallac Victor^2 1420 multilabel plate reader (Perkin Elmer), using the time-resolved fluorescence setting for europium.

Total phosphorylated α-syn (pS-α-syn)

The antibody-sandwich ELISA for total α-syn was modified to detect only the protein phosphorylated at Ser-129 by replacing the 211 phospho-independent capture antibody with polyclonal anti-α-synuclein N-19 (Santa Cruz Biotechnology), diluted 1:3,000 (0.07 μg/ml). The phospho-dependent rabbit monoclonal antibody, Phospho (pS129) antibody (Epitomics), used at a dilution of 1:3000, was the chosen detection antibody. This antibody detects only α-syn phosphorylated at Ser-129. The preferred secondary antibody was human serum absorbed goat anti-rabbit HRP, 1:3000 (KPL), rehydrated in 1 ml H_2O. Recombinant pS-α-syn was used as the assay standard.

Oligomeric phosphorylated α-syn (oligo-pS-α-syn)

The antibody-sandwich immunoassay for oligo-α-syn was modified to detect only phosphorylated, oligomeric forms of the

protein, by replacing the 211 phospho-independent capture antibody with the phospho-dependent rabbit monoclonal antibody, pS129 (Epitomics), used at a dilution of 1:3000. The detection antibody was biotinylated pS129 at a dilution of 1:400. Recombinant oligo-pS-α-syn was used to generate a standard curve.

Preparation of biotinylated antibodies

To prepare the biotinylated antibody, 200 g Sulfo-NHS-LC-Biotin (Pierce, Rockford, IL, USA) was reacted with the required antibody (1 ml, 200 μg/ml) in PBS and then placed on ice for 2 h. The mixture was desalted on Bio-Spin-6 columns (Bio-Rad, Richmond, CA, USA) to remove excess uncoupled biotin and the biotinylated antibody was stored at −20°C until use.

Immunocapture of α-syn from plasma

Dynabeads covalently coupled with recombinant protein G were derivatized with goat polyclonal anti-α-syn synuclein N-19 antibody (Santa Cruz Biotechnology), as recommended by the manufacturer (Dynal Biotech, Wirral, UK). Plasma (500 μl) was added to the beads and incubated overnight at 4°C. The plasma samples were chosen according to the immunoassay results, with one sample giving a high signal for the phosphorylated protein, the other a low signal, and a control containing PBS only. The beads were then washed 3 times with 0.1 M phosphate buffer (pH 8.2). Any captured protein was eluted from the beads by boiling for 10 min in NuPAGE LDS sample buffer (Invitrogen, Carlsbad, CA, USA) and was examined by gel electrophoresis and immunoblotting.

Gel electrophoresis and immunoblotting

The protein eluted from the magnetic Dynabeads was separated on 12.5% acylamide gels. The separated proteins were transferred to nitrocellulose membranes (0.45 μm, Invitrogen) at 30 V, 125 mA for 1 h. Membranes were blocked with 5% dried skimmed milk dissolved in PBS-Tween (PBST), for 1 h. The membranes were probed overnight at 4°C with either phospho-dependent rabbit anti-α-synuclein monoclonal antibody pS129 (Epitomics) at a dilution of 1:5000; rabbit polyclonal anti-synuclein antibody FL-140 (Santa Cruz Biotechnology) at a dilution of 1:1000 (0.2 μg/ml); or rabbit anti-ubiquitin antibody FL-76 (Santa Cruz Biotechnology) at a dilution of 1:1000 (0.2 μg/ml) in PBST. The membranes were washed 3 times in PBST, followed by incubation with human serum absorbed HRP-conjugated goat anti-rabbit (Sigma), 1:10,000 in PBST, for 1 h. The protein bands were visualized using ECL reagents (Pierce), as described by the manufacturer.

Analysis of immunoassay data

A set of standards for one of the 4 different assays (*i.e.*, for total α-syn, oligo-α-syn, pS-α-syn, or oligo-pS-α-syn) was included on each microtiter plate, as appropriate for the type of protein being measured on that plate. Standard curves were fitted using nonlinear least squares (see **Fig. 1** for representative examples of standard curves for each of the four different immunoassays). The samples of blood plasma from

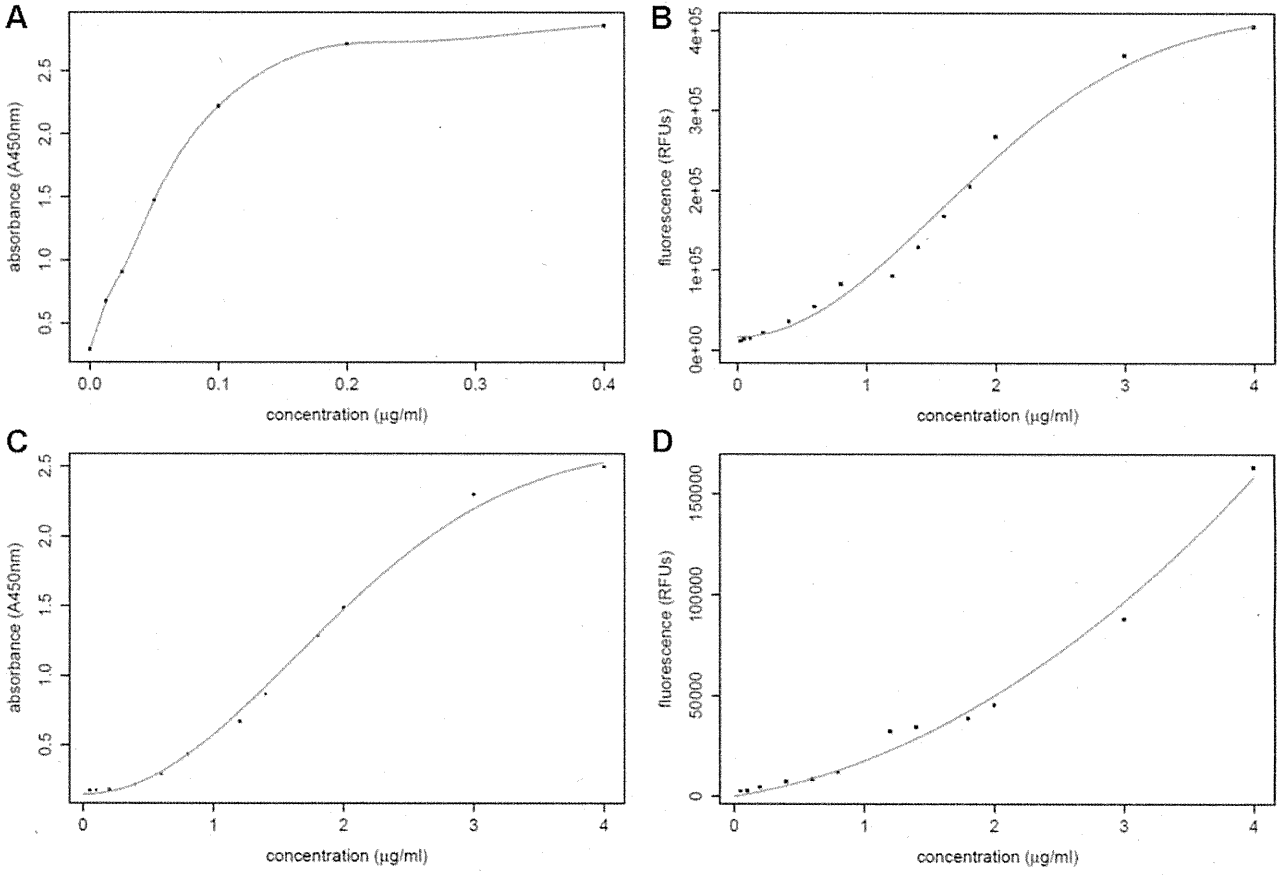

Figure 1. Examples of standard curves obtained for total α-syn (*A*), oligo-α-syn (*B*), pS-α-syn (*C*) and oligo-pS-α-syn (*D*). These are representative curves, each obtained from a single ELISA plate.

patients with PD and controls, diluted as indicated above, were measured in triplicate for each individual at each time point. The standard curves for each individual plate were used to transform the absorbance values (total α-syn, pS-α-syn) or relative fluorescence units (RFU; oligo-α-syn, oligo-pS-α-syn) for that particular plate into protein concentrations, and, in this way, any variation between plates was accounted for. The specificity of the oligo-α-syn immunoassay toward aggregated forms of α-syn has been reported previously (37, 41) but was confirmed here by analysis of fractions obtained by gel filtration of preaggregated, recombinant α-syn; only the peak containing α-syn oligomers, and not the monomer peak, was detected by the oligo-α-syn immunoassay. Also, as expected, the nonphosphorylated form of α-syn gave no signal in the pS-α-syn immunoassay, and the oligo-pS-α-syn immunoassay detected only pS-α-syn that had been preaggregated (data not shown). Further, when the blood plasma samples were immunodepleted with anti-α-syn antibodies C211 or FL-140, each coupled to magnetic Dynabeads, and then tested in the immunoassays, only trace signals could be detected above background compared to the nonimmunodepleted samples (data not shown).

To investigate whether the protein levels changed over time (*i.e.*, during the first 3 mo) a linear mixed model was fitted to the longitudinal data from each assay (details in Supplemental Data).

A classic 2-sample *t* test was used to determine whether there was any significant difference between the mean levels of each of the different forms of α-syn when comparing the plasma samples from the patients with PD with those from the healthy controls. To better satisfy the assumptions underlying this test, the empirical distributions were constructed on the logarithmic scale to obtain a more symmetric distribution than was obtained on the original scale.

RESULTS

Patient population and demographics

Demographic details of the cohort of 32 patients with PD that was followed at monthly intervals for 3 mo are summarized in **Table 1**. The mean age of this cohort on ascertainment and initial sampling was 68.2 yr (youngest 56 yr, oldest 85 yr). Among the 30 recruited healthy controls, there were 13 males and 17 females, with a median age of 63 yr and mean age of 61.5 yr (youngest 42 yr, oldest 75 yr). The PD case and control subjects were recruited in parallel, at the same clinical centers, and the blood samples were taken and processed by the same personnel at each site. Moreover, the plasma samples were effectively randomized for analysis, with both control and PD samples being assayed together on the same microtiter plates.

TABLE 1. *Demographic details of the cohort of 32 patients with PD*

Parameter	Value
Gender (male/female)	23/9
Hoehn and Yahr 1.0	5
Hoehn and Yahr 1.5	3
Hoehn and Yahr 2.0	24
Median PD onset age (yr)	61.9 (55.5–69.7)
Age at study recruitment (yr)	68.4 (62.3–73.8)
Disease duration at study recruitment (yr)	4.9 (3.1–9.3)

Values in parentheses indicate interquartile range.

Longitudinal data from patients with PD

Figure 2 presents a bar plot of the total α-syn plasma concentrations for each individual with PD over time (*i.e.*, for mo 0, 1, 2, 3) where, within each time point, we have averaged over triplicate measurements. It can be seen that the levels of total α-syn varied greatly between individuals, within an overall range of 0.01–6 μg/ml. Although a few individuals did show small, stepwise increases or decreases of total α-syn levels over this (very short) sampling period (see, for example, patient 32 in Fig. 2*B*), one of the most striking findings from this study was that, overall, the immunoassay results from the repeat PD plasma samples were remarkably consistent within each individual over time. This was a general finding for the results from all four of the different α-syn immunoassays, but it is illustrated here (Fig. 2) for the total-α-syn data only. Data for the other 3 assays (Supplemental File S2), together with a linear mixed model-based analysis (Supplemental File S1) for all 4 α-syn assays, are available in Supplemental Data. From the latter analysis, it is clear that the variation in α-syn levels across time within an individual is negligible relative to the variation across individuals. The model specifies a time trend, in addition to accounting for inherent differences in protein levels between individuals and differences across time within an individual. In all cases, the confidence interval for the estimated temporal effect covered 0. Thus, we conclude that there was no significant change over time for the levels of α-syn being measured by any of the immunoassays.

Comparison of patients with PD and controls

Empirical distributions of the α-syn concentrations for each assay were highly skewed on the original scale. **Figure 3** presents box plots pertaining to each assay, stratified according to patients with PD and controls. Note that the whiskers of the box plots extend by no more than the range of the data (largest minus smallest value) multiplied by the interquartile range. Extending the whiskers to the largest and smallest values would yield a rather compressed box. An apparent feature of the box plots is that the median concentration of α-syn for the patients exceeds that of the controls for both of the assays for phosphorylated α-syn (*i.e.*, pS-α-syn in Fig. 3*B*, and oligo-pS-α-syn in Fig. 3*D*). The reverse is true regarding the nonphosphorylated assays (total-α-syn in Fig. 3*A* and oligo-α-syn in Fig. 3*C*). Further, the interquartile range (*i.e.*, box height) reports that the concentrations are far less dispersed for controls compared to patients for both of the phosphorylated α-syn assays. For the nonphosphorylated assays, the controls display a larger spread of concentrations.

To investigate the potential of α-syn as a means of

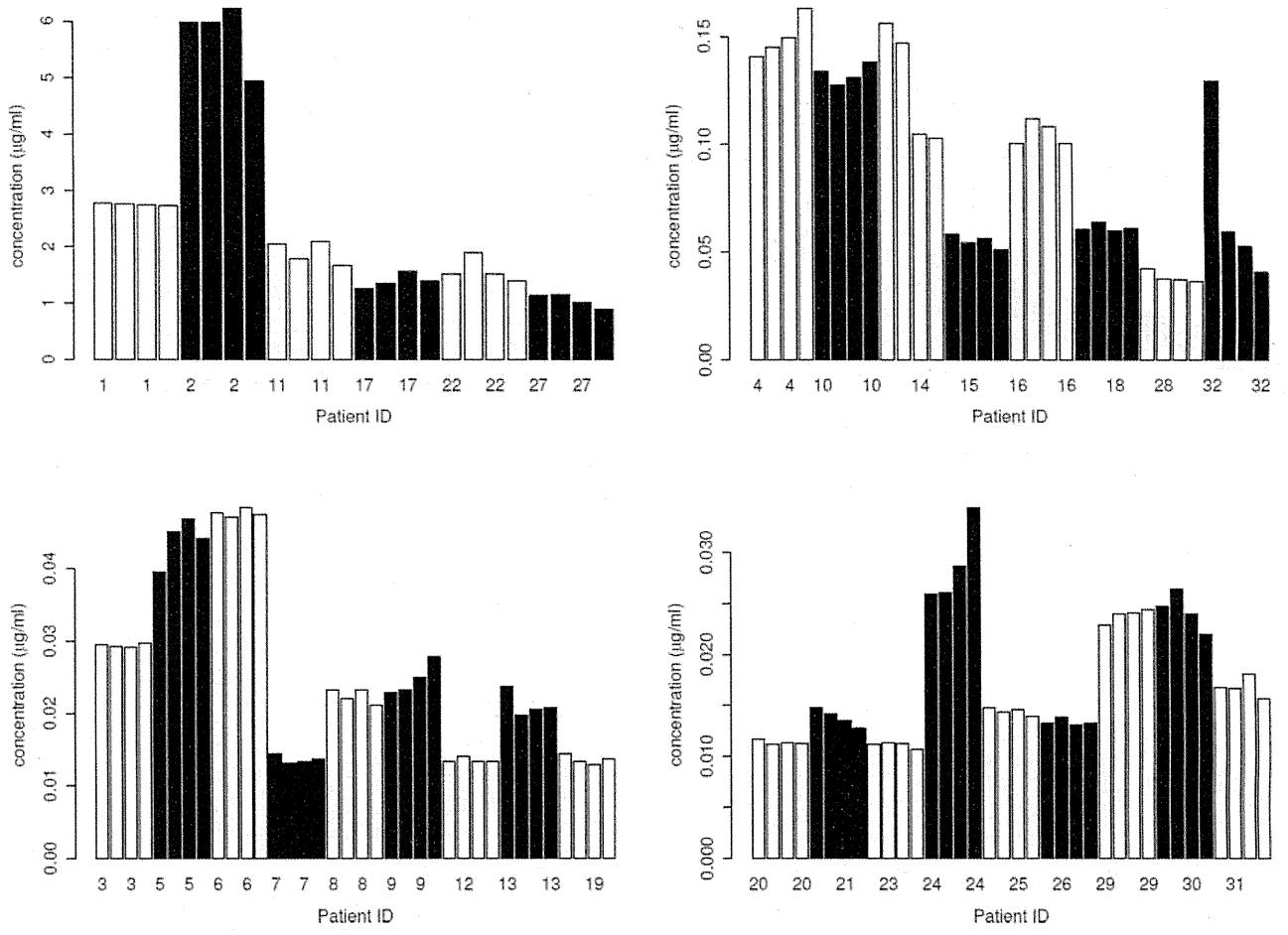

Figure 2. Longitudinal data for the levels of total α-syn in plasma samples from all of the 32 patients with PD. Consecutive bars for each patient represent the level of total α-syn in blood plasma samples taken at 0, 1, 2 and 3 mo. The participants are assigned to one of the 4 sections depending on their overall levels of protein.

discriminating between patients with PD and controls, we determined whether there was any significant difference between the average level of α-syn (on the logarithmic scale) across patients and controls, within all 4 α-syn assays. Because there was no consistent change in α-syn levels over time, nor across replicates within time, in the plasma samples from patients with PD, the concentrations for mo 0, 1, 2 and 3 were averaged over time and replicates in order to obtain a single mean value for each individual patient. Under a classical two-sample *t* test, the mean level of pS-α-syn was found to be marginally significantly higher for the patients than for the healthy controls (P=0.053). On the other hand, there was no difference across the average levels of patients and controls with regard to total α-syn (P=0.244), oligo-α-syn (P=0.221), or oligo-pS-α-syn (P=0.181).

Association with gender and age

The levels of α-syn showed no association with gender. For the total and oligo-α-syn assays, sampling age was a marginally significant −0.049 (−0.099, −0.001; P=0.052) and significant −0.009 (−0.019, −0.001; P=0.045) predictor, respectively, of α-syn levels in the patients with PD. On the other hand, the P values corresponding to the effect of sampling age on α-syn levels in the patients, under the pS-α-syn and oligo-pS-α-syn assays, were 0.412 and 0.274, respectively. The levels of α-syn showed no correlation with age in the control group. We did also analyze the data adjusting for age, but found no significant effects, and the adjustments did not materially change the (lack of) significance of the relevant assay results. Therefore, we chose to report the unadjusted results for simplicity.

Receiver operating curve (ROC) analysis

Figure 4 displays an ROC curve constructed to evaluate the utility of plasma pS-α-syn levels in discriminating patients with PD from healthy controls. The area under the curve (AUC) of 0.68 suggests that pS-α-syn has some potential value as a discriminant between patients and controls. AUC curves for 2 of the other 3 assays gave AUC values of less than 0.5 (0.28 for total α-syn and 0.22 for oligo-α-syn), which would also indicate a potentially informative result, with plasma levels of these being lower in patients than in controls. An AUC of 0.62 for oligo-pS-α-syn, however, suggests that in this

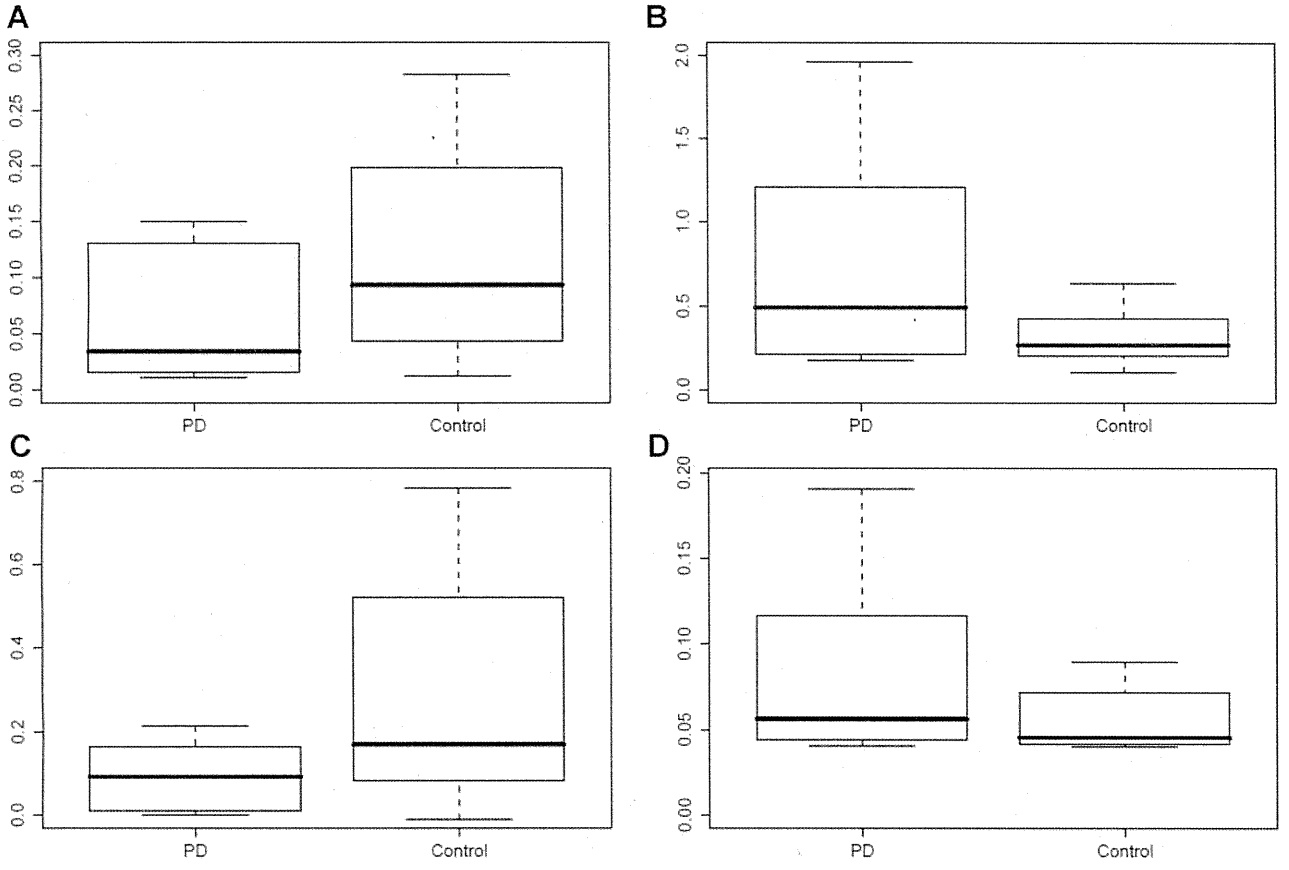

Figure 3. Box plots comparing the levels (in μg/ml) of total α-syn (*A*), pS-α-syn (*B*), oligo-α-syn (*C*), and oligo-pS-α-syn (*D*) in patients with PD compared to healthy controls. In each plot, the box extends from the lower to the upper quartile of the data, with the median indicated by a horizontal line within the box. The difference between the lower and upper quartiles is called the interquartile range (IQR). The upper and lower whiskers extend to the most extreme data values that are no more than 1.5 IQR greater than the upper quartile, and no more than 1.5 IQR less than the lower quartile, respectively.

particular sample set, this assay is less likely to have any practical value as a discriminatory diagnostic tool.

Immunoblot analysis of phosphorylated α-syn in plasma

To better characterize the phosphorylated α-syn detected in plasma, we extracted α-syn from individual PD plasma samples by immunocapture on magnetic Dynabeads and then analyzed the extracted proteins by immunoblotting. The beads were derivatized with the phosphorylation-independent α-syn antibody N-19 (Santa Cruz Biotechnology), which is the antibody used for capture in the pS-α-syn immunoassay. Proteins eluted from the beads were detected by immunoblotting with two different α-syn antibodies: phosphorylation-dependent rabbit monoclonal antibody, pS129, which is the detection antibody used in the pS-α-syn immunoassay (**Fig. 5*A***), and the phosphorylation-independent rabbit polyclonal antibody, FL-140 (Fig. 5*B*). Rabbit anti-ubiquitin antibody FL-76 (Santa Cruz Biotechnology) was used to determine whether any of the bands represented ubiquitinated forms of α-syn (Fig. 5*C*).

The plasma samples were chosen according to the immunoassay results, with one sample giving a low signal for pS-α-syn (Fig. 5, lane 2) and the other a high signal (Fig. 5, lane 3). Immunoblots using the phospho-α-syn-dependent antibody revealed immunoreactive bands from both of these plasma samples, together with the human recombinant phospho-α-syn (at ~17 kDa), but not the nonphosphorylated recombinant protein (Fig. 5*A*, lane 4). The sample derived from the high-reading plasma revealed more intense bands than the low-reading sample, at ~21, 24, and 50–60 kDa. FL-140 revealed both the phosphorylated and nonphosphorylated recombinant protein standards, and also a 24-kDa band in both plasma samples (Fig. 5*B*). The 21-kDa band detected by pS129 was absent, but an additional higher-molecular-weight smear, at >35 kDa, was present. On the basis of the size of these α-syn species, we hypothesize that the 24-kDa band may correspond to phosphorylated, monoubiquitinated α-syn. The anti-ubiquitin antibody, FL-76, strongly labeled the 24-kDa band, as well as the broad "smears" at higher molecular mass, suggesting that all of these bands represent ubiquitinated forms of α-syn (Fig. 5*C*). Control samples of 100 ng human IgG and albumin, the N-19 immunocapture antibody, and a control immunoprecipitation

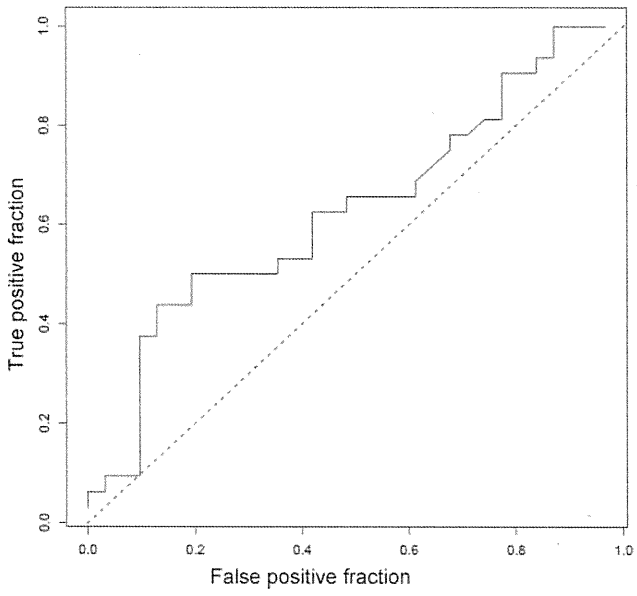

Figure 4. ROC curve showing the ability of the pS-α-syn levels to discriminate between patients with PD and healthy controls (AUC=0.68).

using PBS rather than plasma, gave no immunoreactive bands (data not shown).

DISCUSSION

α-Syn has been linked directly to the etiology of the α-synucleinopathies by mutations in and multiplication of its gene (*SNCA*) that result in familial forms of either PD or DLB. We have reported previously that α-syn is released from cells and is present in human body fluids, including CSF and blood plasma (26). This has led to considerable interest in α-syn in these body fluids as a potential biomarker for the α-synucleinopathies (30–37, 42–44). However, most of these studies have relied on immunoassays that cannot distinguish between monomeric/oligomeric and nonphosphorylated/phosphorylated forms of the protein, apart from two previous studies of oligomeric α-syn in human CSF or blood plasma (37, 44). Here, we have set up individual sandwich immunoassays that can distinguish between total α-syn (MAb 211 capture/ FL-140 detect); oligo-α-syn (Mab 211 capture and detect); pS-α-syn (N19 capture/pS129 detect); and oligo-pS-α-syn (pS129 capture and detect). Our assays for oligomeric forms of α-syn use the double-antibody approach, where the same monoclonal antibody is used for both antigen capture and detection (37, 41). This type of assay cannot detect monomers because the capture antibody occupies the only antibody-binding site available, but it can detect oligomers, because they have multiple binding sites. Our assays for phosphorylated α-syn rely on the specificity of the monoclonal antibody pS129 to α-syn phosphorylated at Ser-129 (45). As anticipated, the recombinant nonphosphorylated α-syn gave no signal in these assays. Although the absorbance/fluorescence values for each of the 4 assays were converted to protein concentrations using the relevant standard curve, due to the nature of these assays, this may only represent an estimate of concentration for that particular assay since the precise nature of the α-syn species detected in plasma has not been not determined for each assay and the native species are likely to differ from the standards prepared from the recombinant

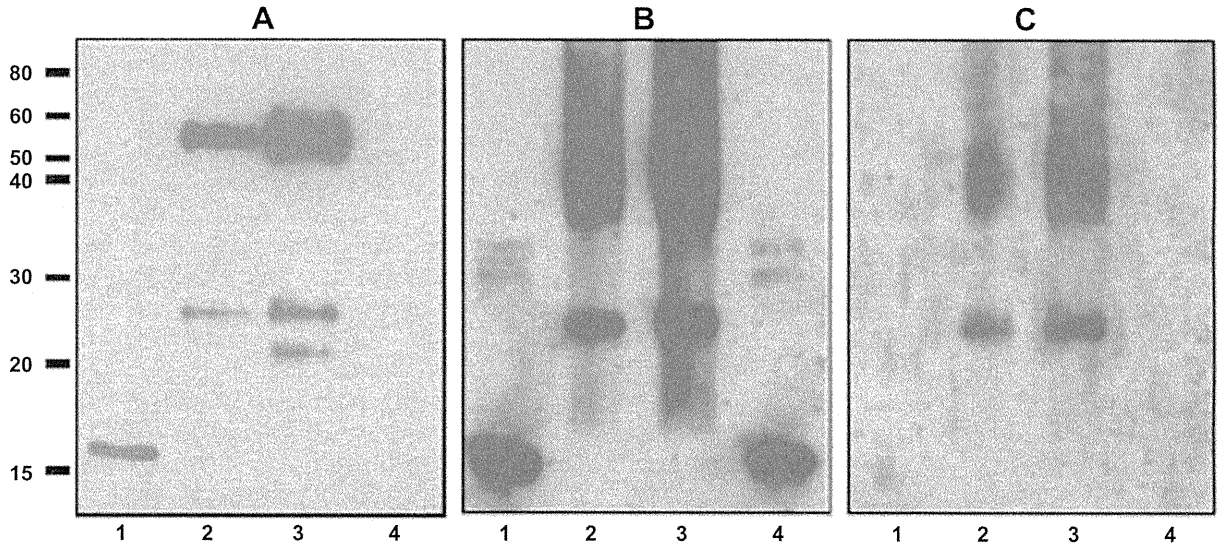

Figure 5. Immunoblot analysis of phosphorylated α-syn from plasma samples. Proteins immunocaptured from one plasma sample giving a low immunoassay signal for pS-α-syn protein (lane 2), and the other a high signal (lane 3), were immunoblotted along with recombinant phosphorylated α-syn (lane 1), and the recombinant nonphosphorylated standard (lane 4). *A*) Analysis with the phospho-dependent α-syn rabbit monoclonal antibody pS129 (Epitomics). *B*) Analysis with the rabbit polyclonal α-syn antibody FL-140 (Santa Cruz Biotechnology). Analysis with the rabbit polyclonal antiubiquitin antibody FL-76 (Santa Cruz Biotechnology).

protein. Nonetheless, the data can be compared within each individual immunoassay, although not necessarily across assays.

As far as we are aware, this is the first report to look at α-syn levels in repeat blood samples taken from individual patients with PD (collected here over an initial 3-mo period, from the first 32 patients enrolled into an ongoing longitudinal study) and also the first to detect phosphorylated forms of α-syn in blood plasma. One of the most important and novel results arising from this study is that although it is clear that the concentrations of α-syn vary greatly between individuals (for reasons that are, as yet, unknown), they remain remarkably consistent (at least over 3 mo) within the vast majority of individuals. This was a general finding for all four of the immunoassays. This lack of fluctuation of α-syn levels within individuals is a prerequisite for establishment of any viable biomarker. It has been reported that only a very small proportion of the α-syn in whole blood is present in peripheral blood mononuclear cells, platelets, and plasma, with the majority being present in red blood cells (46). Considering the abundance and fragility of red blood cells, α-syn levels in plasma, or other bodily fluids, such as CSF, could be artificially elevated in some samples by contamination with intact or lysed red blood cells (32). However, this type of contamination cannot be a confounding factor here, given the very high degree of consistency of α-syn concentrations within the plasma samples prepared from blood taken on 4 different occasions from the same individual. Moreover, it is unlikely that conditions, such as anemia would confound the results because all recruits with PD had undergone regularly blood screening for hemoglobin levels, and if anemia had been detected, it would have been treated.

The results of the 4 different immunoassays reveal that there was, statistically, no difference between the levels of total α-syn, oligo-α-syn, or oligo-pS-α-syn when comparing the 32 patients with PD with the healthy (nondiseased) control group of 30 individuals. This is not consistent with our previous findings for oligo-α-syn (37), which was elevated in PD. However, in our previous study, the control samples were obtained from individuals with serious medical conditions, such as stroke, heart disease, and cancer, and they were also taken at a different institution from the PD samples. In our current study, the controls were from healthy people, and variables such as the collection, separation and storage of the blood samples were more stringently controlled for. It should be noted that the oligo-α-syn immunoassay is the same as that reported in our previous publication (37), except for the detection system, which was changed from alkaline phosphatase (absorbance-based assay) to streptavidin-europium (time-resolved fluorescence). This has improved assay sensitivity and has allowed us to dilute the plasma samples to 1:25, whereas previously (37), the samples were not diluted. It is possible that this has also contributed to the different findings reported here. We now find that only the levels of pS-α-syn were higher in the PD group than in the control group (P=0.053), suggesting that the total phosphorylated protein may be the more useful diagnostic marker in plasma, and this is reflected in the ROC analysis for pS-α-syn (AUC=0.68). It should be noted that we did not make any formal adjustment for multiple testing (Bonferroni correction), because this is only a small-scale study, and this question will be addressed more fully in later work, when we have acquired and analyzed data from many more subjects.

The immunoblot results confirm that immunoreactive protein bands, with an intensity compatible with the immunoassay results, are detected when the protein from plasma is immunocaptured with N-19 and detected on immunoblots with pS129 (*i.e.*, the same capture and detection antibodies as those used for the pS-α-syn immunoassay). Some of these bands seem to represent ubiquitinated forms of the protein, since they also reacted with an antiubiquitin antibody. Whether these phosphorylated and ubiquitinated forms of α-syn originate from a cellular component in the blood itself or whether they originate from a peripheral tissue source elsewhere in the body, or from the brain (*via* CSF) is currently unknown.

Phosphorylation and ubiquitination are important secondary modifications of α-syn, with the protein deposited in LBs being predominantly phosphorylated at serine 129 (3, 47). Ubiquitination is a means of targeting a protein for destruction *via* the proteasome, and a defect in the ubiquitin-proteasome system is likely to be fundamental to the molecular pathogenesis of PD (48), although, recently, it has been suggested that α-syn phosphorylated at Ser-129 is targeted to the proteasome in a ubiquitin-independent manner (49). Phosphorylation of α-syn has been found to promote fibril formation, suggesting that hyperphosphorylation of α-syn might be a contributing factor in the pathogenesis of PD (47, 50). It has also been suggested that α-syn phophorylated at serine 129 and its aggregation are involved in pathway responsible for α-syn toxicity in oligodendrocytes (51, 52). Given this pathological role for phosphorylated and ubiquitinated forms of α-syn, the levels of these modified proteins in body fluids, including blood plasma, are more likely to reflect the fundamental neuropathology of PD than the normal protein (33). This inference is borne out by the results of the present study. Observations that 10–37% of aged, neurologically healthy controls display some α-syn pathology in their brains (53, 54), with about half of such subjects showing abundant α-syn pathology (53), could explain why the levels of pS-α-syn did not better discriminate between patients with PD and healthy controls.

It is also worth noting that the levels of the nonphosphorylated protein in plasma showed a weak but positive correlation with sampling age (of the patients with PD) in the present study, whereas the phosphorylated protein showed no such correlation. Age has already been noted as a confounding variable for total α-syn levels in CSF (32). This lack of correlation between

phosphorylated α-syn and age could be an additional advantage in its development as a potential molecular biomarker.

In summary, we have validated some novel assays for assessing α-syn levels in blood plasma; shown that these levels are highly consistent in repeat blood samples taken over 3 mo from patients with PD; presented evidence for the presence of pS-α-syn (phosphorylated at Ser-129) in blood plasma; and found that the mean level of pS-α-syn was marginally significantly higher (P=0.053) in the PD samples than in the controls. We accept that the latter result is preliminary and will need to be confirmed in larger-scale studies. Nevertheless, on the basis of the data presented here, further study of phosphorylated α-syn as a potential biomarker for PD and related α-synucleinopathies is clearly warranted. Moreover, whether any of the different forms of α-syn can be used to monitor the progression of PD cannot be determined from the present study with longitudinal sampling over 3 mo only and must await data from our ongoing longer-term longitudinal studies. FJ

The authors dedicate this paper to the memory of Prof. John Douglas Mitchell. The authors are grateful to the UK Medical Research Council for financial support (grant award G0601364). The authors thank all of the medical, nursing, and administrative staff of Dementias and Neurodegenerative Diseases Research Network North West, who assisted with the recruitment of patients and the collection and preparation of samples. We also wish to acknowledge and thank all the Consultant Neurologists and their staff within the North West Region of Great Britain who took part in this study, particularly Prof. J. Barrett (Arrowe Park Hospital, Wirral) and Drs. M. Kellett (Salford Royal Hospitals National Health Service Foundation Trust), S. N. H. Naqvi (Chorley and South Ribble District General Hospital), J. Raw (Fairfield General Hospital, Bury), M. J. Steiger (The Walton Centre, Liverpool), P. Tidswell (Royal Blackburn Hospital), C. J. Turnbull (Arrowe Park Hospital, Wirral), and J. Vassallo (Royal Oldham Hospital), for their enthusiasm for, and commitment to, the project. The authors thank students H. Sheldon, S. Macari, E. Mooney, and H. Kennedy from Lancaster Girls Grammar School for their help with the immunoblotting, and Mrs K. Lamb for her assistance in preparing the recombinant proteins.

REFERENCES

1. Spillantini, M. G., Schmidt, M. L., Lee, V. M., Trojanowski, J. Q., Jakes, R., and Goedert, M. (1997) α-Synuclein in Lewy bodies. *Nature* **388,** 839–840
2. Spillantini, M. G., Crowther, R. A., Jakes, R., Hasegawa, M., and Goedert, M. (1998) α-Synuclein in filamentous inclusions of Lewy bodies from Parkinson's disease and dementia with Lewy bodies. *Proc. Natl. Acad. Sci. U. S. A.* **95,** 6469–6473
3. Anderson, J. P., Walker, D. E., Goldstein, J. M., de Laat, R., Banducci, K., Caccavello, R. J., Barbour, R., Huang, J., Kling, K., Lee, M., Diep, L., Keim, P. S., Shen, X., Chataway, T., Schlossmacher, M. G., Seubert, P., Schenk, D., Sinha, S., Gai, W. P., and Chilcote, T. J. (2006) Phosphorylation of Ser-129 is the dominant pathological modification of α-synuclein in familial and sporadic Lewy body disease. *J. Biol. Chem.* **281,** 29739–29752
4. Chartier-Harlin, M. C., Kachergus, J., Roumier, C., Mouroux, V., Douay, X., Lincoln, S., Levecque, C., Larvor, L., Andrieux, J., Hulihan, M., Waucquier, N., Defebvre, L., Amouyel, P., Farrer, M., and Destee, A. (2004) α-Synuclein locus duplication as a cause of familial Parkinson's disease. *Lancet* **364,** 1167–1169
5. Ibáñez, P., Bonnet, A. M., Débarges, B., Lohmann, E., Tison, F., Pollak, P., Agid, Y., Dürr, A., and Brice, A. (2004) Causal relation between α-synuclein gene duplication and familial Parkinson's disease. *Lancet* **364,** 1169–1171
6. Singleton, A. B., Farrer, M., Johnson, J., Singleton, A., Hague, S., Kachergus, J., Hulihan, M., Peuralinna, T., Dutra, A., Nussbaum, R., Lincoln, S., Crawley, A., Hanson, M., Maraganore, D., Adler, C., Cookson, M. R., Muenter, M., Baptista, M., Miller, D., Blancato, J., Hardy, J., and Gwinn-Hardy, K. (2003) α-Synuclein locus triplication causes Parkinson's disease. *Science* **302,** 841
7. Polymeropoulos, M. H., Lavedan, C., Leroy, E., Ide, S. E., Dehejia, A., Dutra, A., Pike, B., Root, H., Rubenstein, J., Boyer, R., Stenroos, E. S., Chandrasekharappa, S., Athanassiadou, A., Papapetropoulos, T., Johnson, W. G., Lazzarini, A. M., Duvoisin, R. C., Di Iorio, G., Golbe, L. I., and Nussbaum, R. L. (1997) Mutation in the α-synuclein gene identified in families with Parkinson's disease. *Science* **276,** 2045–2047
8. Krüger, R., Kuhn, W., Müller, T., Woitalla, D., Graeber, M., Kösel, S., Przuntek, H., Epplen, J. T., Schöls, L., and Riess, O. (1998) Ala30Pro mutation in the gene encoding α-synuclein in Parkinson's disease. *Nat. Genet.* **18,** 106–108
9. Zarranz, J. J., Alegre, J., Gómez-Esteban, J. C., Lezcano, E., Ros, R., Ampuero, I., Vidal, L., Hoenicka, J., Rodriguez, O., Atarés, B., Llorens, V., Gomez Tortosa, E., del Ser, T., Muñoz, D. G., and de Yebenes, J. G. (2004) The new mutation, E46K, of α-synuclein causes Parkinson and Lewy body dementia. *Ann. Neurol.* **55,** 164–173
10. Volles, M. J., and Lansbury, P.T. Jr. (2003) Zeroing in on the pathogenic form of α-synuclein and its mechanism of neurotoxicity in Parkinson's disease. *Biochemistry* **42,** 7871–7878
11. Kayed, R., Head, E., Thompson, J. L., McIntire, T. M., Milton, S. C., Cotman, C. W., and Glabe, C. G. (2003) Common structure of soluble amyloid oligomers implies common mechanism of pathogenesis. *Science* **300,** 486–489
12. Masliah, E., Rockenstein, E., Veinbergs, I., Mallory, M., Hashimoto, M., Takeda, A., Sagara, Y., Sisk, A., and Mucke, L. (2000) Dopaminergic loss and inclusion body formation in α-synuclein mice: implications for neurodegenerative disorders. *Science* **287,** 1265–1269
13. Kahle, P. J., Neumann, M., Ozmen, L., Müller, V., Odoy, S., Okamoto, N., Jacobsen, H., Iwatsubo, T., Trojanowski, J. Q., Takahashi, H., Wakabayashi, K., Bogdanovic, N., Riederer, P., Kretzschmar, H. A., and Haass, C. (2001) Selective insolubility of α-synuclein in human Lewy body diseases is recapitulated in a transgenic mouse model. *Am. J. Pathol.* **159,** 2215–2225
14. Giasson, B. I., Duda, J. E., Quinn, S. M., Zhang, B., Trojanowski, J. Q., and Lee, V. M. (2002) Neuronal α-synucleinopathy with severe movement disorder in mice expressing A53T human α-synuclein. *Neuron* **34,** 521–533
15. Lo Bianco, C., Ridet, J. L., Schneider, B. L., Deglon, N., and Aebischer, P. (2002) α-Synucleinopathy and selective dopaminergic neuron loss in a rat lentiviral-based model of Parkinson's disease. *Proc. Natl. Acad. Sci. U. S. A.* **99,** 10813–10818
16. Irvine, G. B., El-Agnaf, O. M. A., Shankar, G. M., and Walsh, D. M. (2008) Protein aggregation in the brain: the molecular basis for Alzheimer's and Parkinson's diseases. *Mol. Med.* **14,** 451–464
17. Savitt, J. M., Dawson, V. L., and Dawson, T. M. (2006) Diagnosis and treatment of Parkinson disease: molecules to medicine. *J. Clin. Invest.* **116,** 1744–1754
18. Suchowersky, O., Reich, S., Perlmutter, J., Zesiewicz, T., Gronseth, G., and Weiner, W. J. (2006) Practice parameter: diagnosis and prognosis of new onset Parkinson disease (an evidence-based review): report of the Quality Standards Subcommittee of the American Academy of Neurology. *Neurology* **66,** 968–975
19. Hughes, A. J., Daniel, S. E., Kilford, L., and Lees, A. J. (1992) Accuracy of clinical diagnosis of idiopathic Parkinson's disease: a clinico-pathological study of 100 cases. *J. Neurol. Neurosurg. Psychiatry* **55,** 181–184
20. Hughes, A. J., Daniel, S. E., and Lees, A. J. (2001) Improved accuracy of clinical diagnosis of Lewy body Parkinson's disease. *Neurology* **57,** 1497–1499
21. Schapira, A. H. V. (1999) Science, medicine, and the future: Parkinson's disease. *Brit. Med. J.* **318,** 311–314

22. De Lau, L. M., Koudstaal, P. J., Hofman, A., and Breteler, M. M. (2006) Subjective complaints precede Parkinson disease: the Rotterdam study. *Arch. Neurol.* **63,** 362–365
23. Brooks, D. J. (2010) Imaging approaches to Parkinson disease. *J. Nucl. Med.* **51,** 596–609
24. Eller, M., and Williams, D. R. (2009) Biological fluid biomarkers in neurodegenerative parkinsonism. *Nat. Rev. Neurol.* **5,** 561–570
25. Wider, C., Foroud, T., and Wszolek, Z. K. (2010) Clinical implications of gene discovery in Parkinson's disease and parkinsonism. *Mov. Disord.* **25**(Suppl. 1), S15–S20
26. El-Agnaf, O. M. A., Salem, S. A., Paleologou, K. E., Cooper, L. J., Fullwood, N. J., Gibson, M. J., Curran, M. D., Court, J. A., Mann, D. M., Ikeda, S., Cookson, M. R., Hardy, J., and Allsop, D. (2003) α-Synuclein implicated in Parkinson's disease is present in extracellular biological fluids, including human plasma. *FASEB J.* **17,** 1945–1947
27. Lee, H. J., Patel, S., and Lee, S. J. (2005) Intravesicular localization and exocytosis of α-synuclein and its aggregates. *J. Neurosci.* **25,** 6016–6024
28. Emmanouilidou, E., Melachroinou, K., Roumeliotis, T., Garbis, S. D., Ntzouni, M., Margaritis, L. H., Stefanis, L., and Vekrellis, K. (2010) Cell-produced α-synuclein is secreted in a calcium-dependent manner by exosomes and impacts neuronal survival. *J. Neurosci.* **30,** 6838–6851
29. Angot, E., and Brundin, P. (2009) Dissecting the potential molecular mechanisms underlying α-synuclein cell-to-cell transfer in Parkinson's disease. *Parkinsonism Relat. Disord.* **15**(Suppl. 3), S143–S147
30. Tokuda, T., Salem, S. A., Allsop, D., Mizuno, T., Nakagawa, M., Qureshi, M. M., Locascio, J. J., Schlossmacher, M. G., and El-Agnaf, O. M. A. (2006) Decreased α-synuclein in cerebrospinal fluid of aged individuals and subjects with Parkinson's disease. *Biochem. Biophys. Res. Commun.* **349,** 162–166
31. Mollenhauer, B., Cullen, V., Kahn, I., Krastins, B., Outeiro, T. F., Pepivani, I., Ng, J., Schulz-Schaeffer, W., Kretzschmar, H. A., McLean, P. J., Trenkwalder, C., Sarracino, D. A., Vonsattel, J. P., Locascio, J. J., El-Agnaf, O. M. A., and Schlossmacher, M. G. (2008) Direct quantification of CSF α-synuclein by ELISA and first cross-sectional study in patients with neurodegeneration. *Exp. Neurol.* **213,** 315–325
32. Hong, Shi, Z., M., Chung, K. A., Quinn, J. F., Peskind, E. R., Galasko, D., Jankovic, J., Zabetian, C. P., Leverenz, J. B., Baird, G., Montine, T. J., Hancock, A. M., Hwang, H., Pan, C., Bradner, J., Kang, U. J., Jensen, P. H., and Zhang, J. (2010) DJ-1 and α-synuclein in human cerebrospinal fluid as biomarkers of Parkinson's disease. *Brain* **133,** 713–726
33. Foulds, P., Mann, D. M. A., Mitchell, J. D., and Allsop, D. (2010) Progress towards a molecular biomarker for Parkinson disease. *Nat. Rev. Neurol.* **6,** 359–361
34. Lee, P. H., Lee, G., Park, H. J., Bang, O. Y., Joo, I. S., and Huh, K. (2006) The plasma α-synuclein levels in patients with Parkinson's disease and multiple system atrophy. *J. Neural Transm.* **113,** 1435–1439
35. Li, Q. X., Mok, S. S., Laughton, K. M., McLean, C. A., Cappai, R., Masters, C. L., Culvenor, J. G., and Horne, M. K. (2007) Plasma α-synuclein is decreased in subjects with Parkinson's disease. *Exp. Neurol.* **204,** 583–588
36. Shi, M., Zabetianb, C. P., Hancocka, A. M., Ginghinaa, C., Honga, Z., and Yearout, D. (2010) Significance and confounders of peripheral DJ-1 and α-synuclein in Parkinson's disease. *Neurosci. Lett.* **480,** 78–82
37. El-Agnaf, O. M. A., Salem, S. A., Paleologou, K. E., Curran, M. D., Gibson, M. J., Court, J. A., Schlossmacher, M. G., and Allsop, D. (2006) Detection of oligomeric forms of α-synuclein protein in human plasma as a potential biomarker for Parkinson's disease. *FASEB J.* **20,** 419–425
38. El-Agnaf, O. M., Walsh, D. M., and Allsop, D. (2003) Soluble oligomers for the diagnosis of neurodegenerative diseases. *Lancet Neurol.* **2,** 461–462
39. Gibb, W. R. G., and Lees, A. J. (1998) The relevance of the Lewy body to the pathogenesis of idiopathic Parkinson's disease. *J. Neurol. Neurosurg. Psychiat.* **51,** 745–752
40. Sasakawa, H., Sakata, E., Yamaguchi, Y., Masuda, M., Mori, T., Kurimoto, E., Iguchi, T., Hisanaga, S., Iwatsubo, T., Hasegawa, M., and Kato, K. (2007) Ultra-high field NMR studies of antibody binding and site-specific phosphorylation of α-synuclein. *Biochem. Biophys. Res. Commun.* **363,** 795–799
41. El-Agnaf, O. M. A., Paleologou, K. E., Greer, B., Abogrein, A. M., King, J. E., Salem, S. A., Fullwood, N. J., Benson, F. E., Hewitt, R., Ford, K. J., Martin, F. L., Harriott, P., Cookson, M. R., and Allsop, D. (2004) A strategy for designing inhibitors of α-synuclein aggregation and toxicity as a novel treatment for Parkinson's disease and related disorders. *FASEB J.* **18,** 1315–1317
42. Duran, R., Barrero, F. J., Morales, B., Luna, J. D., Ramirez, M., and Vives, F. (2010) Plasma α-synuclein in patients with Parkinson's disease with and without treatment. *Mov. Disord.* **25,** 489–493
43. Reesinka, F. E., Lemstraa, A. W., van Dijka, K. D., Berendsea, H. W., van de Bergb, W. D. J., Klein, M., Blankensteind, M. A., Scheltensa, P., Verbeekf, M. M., and van der Fliera, W. M. (2010) CSF α-synuclein does not discriminate dementia with Lewy bodies from Alzheimer's disease. *J. Alzheimers Dis.* **22,** 87–95
44. Tokuda, T., Qureshi, M. M., Ardah, M. T., Varghese, S., Shehab, S. A., Kasai, T., Ishigami, N., Tamaoka, A., Nakagawa, M., and El-Agnaf, O. M. A. (2010) Detection of elevated levels of α-synuclein oligomers in CSF from patients with Parkinson disease. *Neurology* **75,** 1766–1772
45. Qing, H., Wong, W., McGeer, E. G., and McGeer, P. L. (2009) Lrrk2 phosphorylates α-synuclein at serine 129: Parkinson's disease implications. *Biochem. Biophys. Res. Commun.* **387,** 149–152
46. Barbour, R., Kling, K., Anderson, J. P., Banducci, K., Cole, T., Diep, L., Fox, M., Goldstein, J. M., Soriano, F., Seubert, P., and Chilcote, T. J. (2008) Red blood cells are the major source of α-synuclein in blood. *Neurodegen. Dis.* **5,** 55–59
47. Fujiwara, H., Hasegawa, M., Dohmae, N., Kawashima, A., Masliah, E., Goldberg, M. S., Shen, J., Takio, K., and Iwatsubo, T. (2002) α-Synuclein is phosphorylated in synucleinopathy lesions. *Nat. Cell Biol.* **4,** 160–164
48. Matsuda, N., and Tanaka, K. (2010) Does impairment of the ubiquitin-proteasome system or the autophagy-lysosome pathway predispose individuals to neurodegenerative disorders such as Parkinson's disease? *J. Alzheimers Dis.* **19,** 1–9
49. Machiya, Y., Hara, S., Arawaka, S., Fukushima, S., Sato, H., Sakamoto, M., Koyama, S., and Kato, T. (2010) Phosphorylated α-synuclein at Ser129 is targeted to the proteasome pathway in a ubiquitin-independent manner. *J. Biol. Chem.* **285,** 40732–40744
50. Takahashi, M., Kanuka, H., Fujiwara, H., Koyama, A., Hasegawa, M., Miura, M., and Iwatsubo, T. (2003) Phosphorylation of α-synuclein characteristic of synucleinopathy lesions is recapitulated in α-synuclein transgenic *Drosophila*. *Neurosci. Lett.* **336,** 155–158
51. Gorbatyuk, O. S., Li, S., Sullivan, L. F., Chen, W., Kondrikova, G., Manfredsson, F. P., Mandel, R. J., and Muzyczka, N. (2008) The phosphorylation state of Ser-129 in human α-synuclein determines neurodegeneration in a rat model of Parkinson disease. *Proc. Natl. Acad. Sci. U. S. A.* **105,** 763–768
52. Paleologou, K. E., Oueslati, A., Shakked, G., Rospigliosi, C. C., Kim, H. Y., Lamberto, G. R., Fernandez, C. O., Schmid, A., Chegini, F., Gai, W. P., Chiappe, D., Moniatte, M., Schneider, B. L., Aebischer, P., Eliezer, D., Zweckstetter, M., Masliah, E., and Lashuel, H. A. (2008) Phosphorylation at Ser-129 but not the phosphomimics S129E/D inhibits the fibrillation of α-synuclein. *J. Biol. Chem.* **283,** 16895–16905
53. Zaccai, J., McCracken, C., and Brayne, C. (2005) A systematic review of prevalence and incidence studies of dementia with Lewy bodies. *Age Ageing* **34,** 561–566
54. Parkkinen, L., Pirtilla, T., and Alafuzoff, I. (2008) Applicability of current staging/categorization of α-synuclein pathology and their clinical relevance. *Acta Neuropathol.* **115,** 399–407

Received for publication February 11, 2011.
Accepted for publication August 4, 2011.

Neurobiology of Disease

Regulation of Mitochondrial Transport and Inter-Microtubule Spacing by Tau Phosphorylation at the Sites Hyperphosphorylated in Alzheimer's Disease

Kourosh Shahpasand,[1] Isao Uemura,[2] Taro Saito,[1] Tsunaki Asano,[3] Kenji Hata,[4] Keitaro Shibata,[5] Yoko Toyoshima,[5] Masato Hasegawa,[6] and Shin-ichi Hisanaga[1]

[1]Laboratory of Molecular Neuroscience, [2]Laboratory of Developmental Program, [3]Laboratory of Cell Genetics, [4]Laboratory of Plant Ecology, Department of Biological Sciences, Tokyo Metropolitan University, Minami-osawa, Hachioji, Tokyo 192-0397, Japan, [5]Department of Life Sciences, Graduate School of Arts and Sciences, The University of Tokyo, Komaba, Tokyo 153-8902, Japan, and [6]Tokyo Metropolitan Institute of Medical Sciences, Department of Neuropathology and Cell Biology, Setagaya-Ku, Tokyo 156-0057, Japan

The microtubule-associated protein Tau is a major component of the neurofibrillary tangles that serve as a neuropathological hallmark of Alzheimer's disease. Tau is a substrate for protein phosphorylation at multiple sites and occurs in tangles in a hyperphosphorylated state. However, the physiological functions of Tau phosphorylation or how it may contribute mechanistically to Alzheimer's pathophysiology are not completely understood. Here, we examined the function of human Tau phosphorylation at three sites, Ser199, Ser202, and Thr205, which together comprise the AT8 sites that mark abnormal phosphorylation in Alzheimer's disease. Overexpression of wild-type Tau or mutated forms in which these sites had been changed to either unphosphorylatable alanines or phosphomimetic aspartates inhibited mitochondrial movement in the neurite processes of PC12 cells as well as the axons of mouse brain cortical neurons. However, the greatest effects on mitochondrial translocation were induced by phosphomimetic mutations. These mutations also caused expansion of the space between microtubules in cultured cells when membrane tension was reduced by disrupting actin filaments. Thus, Tau phosphorylation at the AT8 sites may have meaningful effects on mitochondrial movement, likely by controlling microtubule spacing. Hyperphosphorylation of the AT8 sites may contribute to axonal degeneration by disrupting mitochondrial transport in Alzheimer's disease.

Introduction

Mitochondrial transport within axons is crucial for axonal maintenance, and its dysregulation can contribute to neurodegenerative diseases (Su et al., 2010). In axons, mitochondrial movement is driven by two oppositely directed motor proteins, kinesin and dynein, along microtubules (MTs) (Hollenbeck and Saxton, 2005; Bereiter-Hahn and Jendrach, 2010). The surface of MTs is decorated with microtubule-associated proteins (MAPs) (Marx et al., 2006; Vershinin et al., 2007). Tau serves as a predominant MAP in axons and is a filamentous protein of 441 amino acid residues (the longest human isoform). Tau is comprised of two functional regions, the N-terminal projection domain that protrudes from the surface of MTs and the C-terminal MT-binding domain. Overexpression of Tau inhibits mitochondrial transport in various cells (Ebneth et al., 1998; Trinczek et al., 1999; Stamer et al., 2002; Dixit et al., 2008; Stoothoff et al., 2009; Vossel et al., 2010). However, the mechanism and regulation of Tau-mediated inhibition of mitochondrial transport are not understood.

Tau is a major component of neurofibrillary tangles found in Alzheimer pathology. Tau is also a phosphoprotein, the functions of which can be regulated by phosphorylation (Stoothoff and Johnson, 2005; Hanger et al., 2009). Many of the phosphorylation sites reside in proline-directed (Ser/Thr)-Pro sequences. These sites are moderately phosphorylated in healthy neurons. However, hyperphosphorylation is linked to neurodegeneration with phosphorylation of more than 20 sites shown in the degenerated brains of Alzheimer's patients (Watanabe et al., 1993; Morishima-Kawashima et al., 1995; Stoothoff and Johnson, 2005). Cdk5 and GSK3β are two proline-directed protein kinases that are known to phosphorylate these (Ser/Thr)-Pro sites (Ishiguro et al., 1992; Planel et al., 2002). Furthermore, hyperactivation of Cdk5 or GSK3β reduces mitochondrial movement (Darios et al., 2005; Morel et al., 2010). However, it has not been clearly demonstrated whether Tau is a major downstream target of these kinases and, if so, which phosphorylation site(s) is critical. Among GSK3β- and Cdk5-related phosphorylation sites, Ser199, Ser202, and Thr205 are particu-

Received Nov. 29, 2011; accepted Dec. 12, 2011.

Author contributions: K. Shahpasand and S.-i.H. designed research; K. Shahpasand performed research; I.U., T.S., T.A., K. Shibata, Y.T., and M.H. contributed unpublished reagents/analytic tools; K. Shahpasand, I.U., T.S., K.H., and S.-i.H. analyzed data; K. Shahpasand and S.-i.H. wrote the paper.

This work was supported by Grants-in-Aid for Scientific Research on Priority Area from MEXT of Japan (S.H). K. S. was supported by JGC-S Scholarship Foundation. We thank Dr. Peter Davies at Albert Einstein College of Medicine for providing MC-1 and Alz-50 monoclonal anti-Tau antibodies. We also thank Miss. Elizabeth Zielinska for reading this paper.

Correspondence should be addressed to either Kourosh Shahpasand or Shin-ichi Hisanaga. Laboratory of Molecular Neuroscience, Department of Biological Sciences, Tokyo Metropolitan University, Minami-osawa 1-1, Hachioji, Tokyo 192-0391, Japan. E-mail: kourosh-shahpasand@ed.tmu.ac.jp or hisanaga-shinichi@tmu.ac.jp.

DOI:10.1523/JNEUROSCI.5927-11.2012

 0270-6474/12/322430-12$15.00/0

larly interesting. These phosphorylated sites are recognized by the phosphorylation-dependent monoclonal antibody AT8 (Goedert et al., 1995; Wang et al., 2006; Hanger et al., 2009), and their detection by this antibody is commonly used as a marker of abnormal phosphorylation in brains of Alzheimer's patients. These sites are located at the border of the projection domain and MT-binding Pro-rich region (see Fig. 1*A*). Phosphorylation at these sites may extend the projection domain outwards from the surface of MTs (Jeganathan et al., 2008) and affect mitochondrial transport (Mukhopadhyay and Hoh, 2001; Jeganathan et al., 2008; Shahpasand et al., 2008).

Here, we directly examined the effect of phosphorylation at the AT8 sites on mitochondrial transport using the nonphosphorylatable Ala mutant (3A) and the constitutive phosphorylation mimic Asp mutant (3D) of Tau. Overexpression of Tau 3D decreased the mitochondrial movement and expanded the inter-MT spacing more than that of wild-type (WT) Tau or Tau 3A. These results suggest that phosphorylation at the AT8 sites affects mitochondrial transport by changing the spaces between MTs.

Materials and Methods

Anti-human Tau (A0024) was obtained from Dako. Anti-phospho-Tau antibody AT8 was purchased from Thermo Scientific. Anti-TOM20 (FL-145) was from Santa Cruz Biotechnology. MC-1 and Alz-50 anti-Tau antibodies were generous gifts from Dr. Peter Davies (Albert Einstein College of Medicine, Bronx, NY). Anti–β-tubulin and latrunculin B were from Sigma-Aldrich. Anti-His tag was from Invitrogen. NGF and Phos-tag acrylamide was obtained from Wako Chemicals.

Construction of expression vectors for Tau proteins. Mutations of Tau at Ser199, Ser202, and Thr205 were introduced in the longest wild-type human Tau in a pSG5 expression vector. Double Ala mutants (2A) at Ser202A and Thr205A were constructed with PCR using primers 5′-GGCGCCCCAGG CGCTCCCGGCAGCCGC-3′ (forward) and 5′-CCGCGGGGTCCGC-GAGGGCCGTCGGCG-3′ (reverse). For Tau 3A, an additional Ala mutation at Ser199 was constructed with PCR using Tau 2A as a template and primers 5′-AGCGGCTACAGCGCCCCCGGCGCCCCA-3′ (forward) and 5′-TCGCCGATGTCGCGGGGGCCGCGGGGT-3′ (reverse). Tau 3D was constructed by one-step PCR using Tau 3A as a template and primers 5′-AGCGGCTACAGCGACCCCGGCGACCCAGGCGATCCCGGCAGC-CGC-3′ (forward) and 5′-TCGCCGATGTCGCTGGGGCCGCTGGGTCC GCTAGGGCCGTCGGCG-3′ (reverse). All constructs were confirmed by DNA sequencing. Bacterial expression vectors encoding Tau 3A and Tau 3D were constructed similarly with PCR using Tau 1N4R (one N-terminal insertion and four MT-binding repeats) in the pRK172 vector. Baculovirus expression vectors for Tau proteins were constructed as follows. Tau WT, 3A, or 3D in pSG5 was amplified with PCR using primers 5′-GGATCCATG-GCTGAGCCCCGCCA-3′ (forward, with BamHI site) and 5′-GCGGC-CGCTCACAAACCCTGCTT-3′ (reverse, with NotI site). PCR products were inserted into the pCR2.1 vector. Tau cDNAs were digested with BamHI and NotI and inserted into pFastBac Dual, the donor vector for the Bac-to-Bac Baculovirus Expression System (Invitrogen). Recombinant plasmids were used to transform competent DH10Bac cells for transposition to the bacmid shuttle vectors. Recombinant bacmid DNA was transfected into monolayers of Sf9 insect cells. Supernatants containing virus were harvested 96 h after transfection, and the viral titer was amplified and determined according the manufacturer's instructions (Invitrogen).

Cell culture and expression of Tau proteins. COS-7 cells (2×10^5 per ml) were grown in DMEM (Sigma) containing 10% FBS and transfected with PolyFect reagent (Qiagen) (Kaminosono et al., 2008).

PC12 cells (2×10^5 per ml) were cultured on 35 mm glass-bottom dishes in DMEM containing 10% FBS and antibiotics (penicillin and streptomycin) at 37°C in 5% CO_2. Cells were treated with NGF (50 ng/ml) 4 h after transfection for 3 d.

Primary neurons were prepared from 17-day-old embryonic mouse brain cerebral cortex of either sex. Neurons (2×10^5 per ml) were seeded on 35 mm glass-bottom dishes. The medium was then changed to neurobasal medium supplemented with B27 (Invitrogen) and 1 mM L-glutamine (Endo et al., 2009). Cells were transiently transfected with Tau WT, 3A, or 3D with Lipofectamine 2000 (Invitrogen). Various amounts of Tau cDNA (1–4 μg) were tested to determine the appropriate amount of cDNA. The levels of Tau expression were quantified by immunostaining intensity as described below. Neurons were cotransfected with Mito-GFP to label and observe mitochondrial movement.

Sf9 cells were grown at 27°C in 35 mm dishes in complete serum-free medium (Invitrogen) and antibiotics (penicillin and streptomycin). Monolayer cultures of Sf9 cells (4×10^5 per ml) were infected with baculoviruses encoding Tau cDNA at a titer of 2×10^7 pfu/ml. Cells were treated with 0.5 μg/ml latrunculin B from the time of infection for 72 h and were fixed with 2.5% glutaraldehyde and 2% PFA in PEM buffer (0.1 M PIPES, pH 7.2, 1 mM EGTA, 1 mM $MgCl_2$) for 30 min at room temperature.

Immunostaining. One day after transfection, COS-7 cells were treated with PEM buffer containing 4 M glycerol and 0.5% Triton X-100 for 10 min at 37°C. After fixation with cold methanol for 3 min, cells were incubated with anti-tubulin (1:500) or anti-Tau (1:500), followed by Alexa Fluor-conjugated anti-mouse IgG or anti-rabbit IgG (1:500).

Sf9 cells, PC12 cells, and cortical neurons cultured on glass coverslips were fixed with 4% PFA in PBS for 20 min and permeabilized with 0.1% Triton X-100 in PBS containing 5% BSA for 20 min. Cells were incubated with anti-Tau (1:500) followed by Alexa Fluor 546-labeled secondary antibody. Immunofluorescent stainings were examined with an LSM5 EXCITER microscope (Zeiss), and fluorescent intensities were measured for 20 processes per sample with ZEN 2008 software (Zeiss). Length and width of Sf9 cell processes were measured for 20 cells per sample with ImageJ software.

Electron microscopy. Sf9 cells were infected with baculovirus encoding Tau constructs and 72 h after infection cells were fixed and processed for electron microscopic observation (Tokuoka et al., 2000). PC12 cells were transfected with plasmids encoding Tau and EGFP. Tau-expressing PC12 cells were identified with EGFP after fixation, and their positions were marked on the base of culture dishes by a felt pen. Fixation was done with 2.5% glutaraldehyde and 2% PFA in PEM buffer (0.1 M PIPES, pH 7.2, 1 mM EGTA, 1 mM $MgCl_2$) for 30 min at room temperature. Specimens were examined with a JEM-1010 transmission electron microscope (JEOL). Inter-MT distances in sections cut perpendicularly to longitudinal axis of MTs were measured with ImageJ software.

Time-lapse imaging and statistical methods. Mitochondrial movement in NGF-treated PC12 cells and mouse brain cortical neurons was examined with an LSM 5 EXCITER microscope using an incubation chamber with 5% CO_2 at 37°C. Fluorescent images of mitochondria in the longest process of each PC12 cell and axons of cortical neurons were acquired at intervals of 5 s over a period of 300 s. In each experiment, eight mitochondria in five cells were analyzed for their movement in image stacks composed of 60 images. Individual mitochondrial movements were analyzed with ZEN 2008 software (Zeiss). Differences in the position of each mitochondrion between two frames during each 5 s interval were exported to Excel, and they were classified and scored as stationary, anterograde, or retrograde movements. Completely immotile mitochondria during 300 s of observation were excluded from the counts. Kymographs were made using serial frames of the same area during the observation period.

Statistical differences in stationary phase of mitochondria among control, Tau WT, 3A, and 3D were analyzed by one-way ANOVA. Holm's multiple test was conducted on all possible pairwise combinations. Differences in the ratios between anterograde and retrograde movements were analyzed by ANCOVA. The dependent variable was time of anterograde movement, and the independent variables were Tau transfection samples as a fixed factor and time of retrograde movement as a covariate. After confirming no interaction between Tau transfection samples and the retrograde ratios, the anterograde/retrograde moving durations were compared using all data or data of Tau-transfected samples. When $p > 0.05$, the difference was considered nonsignificant. All of the statistical analyses were carried out with version 2.13.1 of the R software package (R: A language and environment for statistical computing. R Development Core Team, Vienna, Austria, 2011, available at http://www.R-project.org).

Protein purification, motor–MT binding assay, and in vitro *phosphorylation of Tau by Cdk5-p25.* Tau WT, 3A, or 3D was expressed in *Escherichia coli* and purified (Sakaue et al., 2005). Porcine brain tubulin was also purified as described (Sakaue et al., 2005). Kinesin RK430-AviTag-KRC-His_6 was expressed and purified from *E. coli* as described (Furuta et al., 2008), except that ATP was not added to the preparation buffers. Tubulin (0.5 μM) was assembled in PEM containing 1 mM GTP and 10 μM Taxol in the presence of various concentrations of Tau WT, 3A, or 3D (0.05, 0.1, or 0.15 μM) and 0.1 μM RK430 at 37°C for 45 min. Polymerized MTs were collected by centrifugation at 100,000 × *g* for 60 min at 37°C. The supernatants and pellets were subjected to SDS-PAGE followed by immunoblotting. Cdk5-p25 was purified from Sf9 cells that had been infected with baculovirus encoding Cdk5 and p25 (Saito et al., 2003). Phosphorylation of Tau by Cdk5-p25 was performed *in vitro* by incubating 50 μg/ml Tau WT, 3D, or 3A with Cdk5-p25 at 37°C for 2 h.

SDS-PAGE and immunoblotting. SDS-PAGE and immunoblotting were performed as described (Sakaue et al., 2005). Phos-tag SDS-PAGE was performed with 7.5% polyacrylamide and 50 μM Phos-tag as described (Hosokawa et al., 2010). Dot blot was performed with MC-1 and Alz-50 antibodies using the method reported previously (Jicha et al., 1997). All experiments were performed at least three times, and representative results are shown.

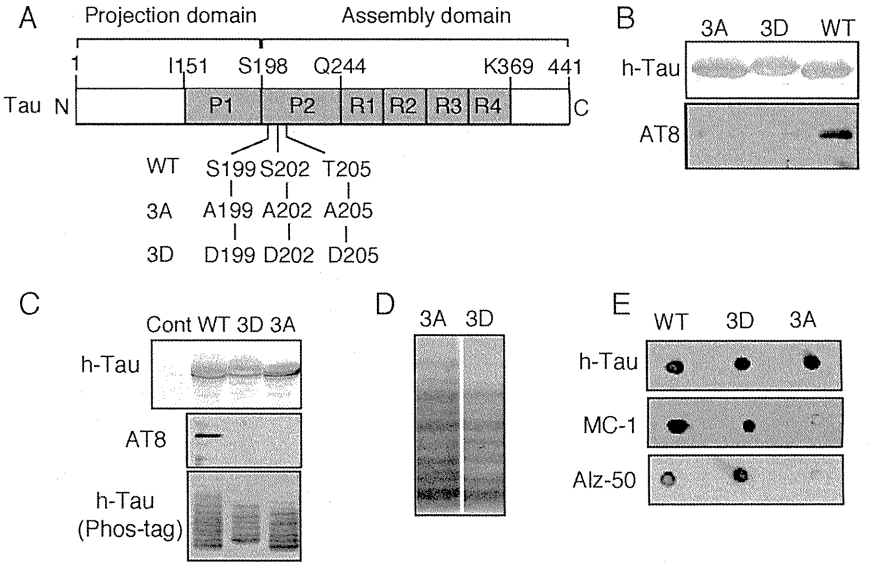

Figure 1. Phospho-mimic mutant of Tau 3D at the AT8 sites Ser199/Ser202/Thr205. ***A***, Schematic representation of the longest human isoform of Tau composed of 441 amino acid residues. Tau consists of the N-terminal projection domain and C-terminal MT-assembly domain including four MT-binding repeats (R1–R4). Two proline-rich regions (P1 and P2) are present in the middle region. The AT8 Ser199/Ser202/Thr205 sites are located in the N-terminal side of P2 at the border of the projection domain and MT-binding domain. This molecular structure was drawn based on the description by Jeganathan et al. (2006). Amino acids that can be phosphorylated were replaced with Asp or Ala to generate the phosphorylation mimic (3D) or nonphosphorylated (3A) Tau constructs, respectively. ***B***, Cdk5-dependent *in vitro* phosphorylation at the AT8 sites of Tau WT, but not Tau 3A or 3D. Tau WT, 3A, and 3D were phosphorylated *in vitro* with Cdk5–p25. Immunoblots were performed with anti-human Tau (h-Tau) or AT8. ***C***, Phosphorylation at the AT8 sites of Tau WT, but not 3A or 3D, in COS-7 cells. Tau WT, 3A, or 3D was expressed in COS-7 cells. Cell lysates were subjected to immunoblotting for h-Tau or AT8. The bottom panel shows evaluation of phosphorylation state-dependent mobility shifts of Tau WT, 3A, or 3D expressed in COS-7 cells by Phos-tag SDS-PAGE. Tau WT, 3A, and 3D separated by Phos-tag SDS-PAGE were immunoblotted with anti-human Tau. Cont, Control. ***D***, Alignment of Tau 3A and 3D to compare their banding patterns in Phos-tag SDS-PAGE. Phos-tag immunoblots of Tau 3A and 3D in ***C*** were aligned by adjusting the fastest moving band. ***E***, Tau 3D takes conformation similar to phosphorylated Tau WT. After *in vitro* phosphorylation of Tau constructs with Cdk5–p25, dot blots were performed with phosphorylation-independent antibody h-Tau (top) and with phosphorylation-dependent antibodies, MC-1 (middle), and Alz-50 (bottom).

Results

Phosphorylation of Tau mutants and their binding to MTs

Tau can be phosphorylated at multiple sites *in vitro* and *in vivo*. To assess the effects of site-specific phosphorylation on mitochondrial transport, we used the Tau mutants 3A (nonphosphorylatable) and 3D (phosphorylation mimic), each of which was mutated at the AT8 Alzheimer phosphorylation sites (Ser199, Ser202, and Thr205) (Fig. 1*A*). Recombinant Tau WT, 3A, and 3D were phosphorylated *in vitro* by Cdk5-p25 and immunoblotted with AT8, which recognizes Tau that is phosphorylated at Ser202 and Thr205 (Goedert et al., 1995) or Ser199, Ser202, and Thr205 (Hanger et al., 2009). Phosphorylated Tau WT was immunoreactive to AT8, whereas phosphorylated Tau 3A and 3D were not (Fig. 1*B*), confirming that Cdk5 indeed phosphorylated the sites recognized by AT8 (Takahashi et al., 2003) and that these phosphorylation sites were disrupted in 3A and 3D constructs. These Tau constructs were expressed in COS-7 cells, and phosphorylation was examined by immunoblotting with AT8. Immunodetection of Tau WT but not 3A nor 3D clearly demonstrated that Tau WT was phosphorylated at the AT8 recognition sites in COS-7 cells (Fig. 1*C*, middle).

To determine whether the mutations affected phosphorylation of Tau at other sites, Tau expressed in COS-7 cells was detected by immunoblotting with a phosphorylation-independent Tau antibody after Phos-tag SDS-PAGE. Phos-tag SDS-PAGE is a recently developed method that detects phosphorylated proteins via an expanded mobility shift on SDS-PAGE (Kinoshita et al., 2006; Hosokawa et al., 2010). Multiple Tau bands indicated the presence of various phosphorylated forms of Tau in COS-7 cells (Fig. 1*C*, bottom). As a whole, the decreased mobility of Tau WT compared to Tau 3A indicated the higher level of phosphorylation of Tau WT, including the AT8 site. The relative upward shift of all the Tau 3D bands was apparently due to the increased negative charge of the three Asp residues at positions 199, 202, and 205. Phosphorylated Tau 3A and 3D had similar, but not identical, banding patterns, suggesting that these mutants underwent similar phosphorylation at other sites (Fig. 1*D*). These results indicated that by using Tau 3A and 3D, we could examine the role of Tau phosphorylation at the AT8 sites (Ser199/Ser202/Thr205) on mitochondrial transport.

To see whether the 3D mutant mimics the phosphorylation state at the AT8 sites, we performed dot blot of Tau constructs with MC-1 and Alz-50 antibodies after phosphorylation with Cdk5-p25. MC-1 and Alz-50 are monoclonal antibodies that recognize conformation of Tau when phosphorylated at both AT8 and PHF-1 (Ser396 and Ser 404) sites (Jicha et al., 1999). Cdk5-phosphorylated Tau WT and Tau 3D, but not Tau 3A, were immunoreactive to MC-1 and Alz-50 (Fig. 1*E*). The results indicated that Tau 3D in fact mimics phosphorylation at the AT8 sites.

To assess Tau 3A and 3D binding to MTs, COS-7 cells were transfected with vectors that mediated expression of WT, 3A, or 3D forms of Tau. The Tau-expressing cells were then incubated in a MT-stabilizing buffer containing 0.5% Triton X-100 and 4 M glycerol to remove soluble tubulin and Tau and then stained with anti-tubulin and anti-Tau (Bershadsky et al., 1978; Kaminosono

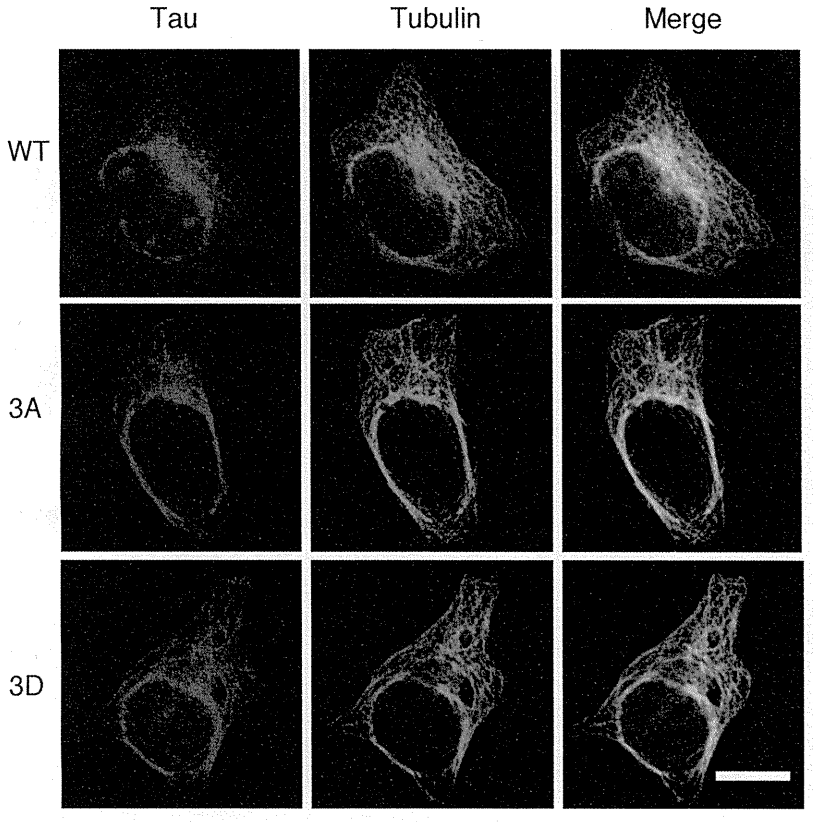

Figure 2. Colocalization of Tau WT, 3A, or 3D to MTs in COS-7 cells. Tau WT, 3A, or 3D vectors were used to transfect COS-7 cells. Soluble Tau and tubulin were removed by treatment with PEM containing 4 M glycerol and 0.5% Triton X-100 for 10 min at 37°C, and cells were double-stained with anti-tubulin (green in middle panels) and anti-Tau (red in left panels), followed by fluorescently labeled secondary antibodies. Merged images are shown in the right panels. Scale bar, 20 μm.

et al., 2008). In all three cases, there was wide codistribution of Tau and MT (Fig. 2), suggesting that Tau phosphorylation at the AT8 sites does not inhibit the binding of Tau to MTs in cells, as reported previously (Rankin et al., 2005; Hanger et al., 2009). Furthermore, *in vitro* studies indicated that both recombinant pure Tau 3A and 3D bound to MTs similarly to Tau WT (data not shown).

Expression of Tau constructs in PC12 cells and cultured cortical neurons

Expression levels of Tau WT, 3A, and 3D in PC12 cells and cultured neurons were measured after immunofluorescent staining. The immunostainings of neurons are shown in Figure 3*A*. The staining intensity increased with concentrations of plasmids from 2 to 3 μg used for transfection (Fig. 3*B*,*C*). When 2.5 μg of plasmids were used, the fluorescent intensities were ~1.7 and ~1.5 fold of untransfected PC12 cells (Fig. 3*B*) and cultured neurons (Fig. 3*C*), respectively. Expression levels were almost similar among Tau WT, 3A, and 3D constructs (Fig. 3*B*,*C*). The effect of Tau on mitochondrial movement was dependent on the amount of Tau plasmid used for transfection. While transfection with less than 2 μg did not significantly affect mitochondrial movement, more than 3 μg had a substantial (and similar) effect for all Tau constructs (data not shown). Differences were observed with 2.5 μg DNA, which was used in subsequent experiments.

Tau phosphorylation reduces mitochondrial motility in neuritic processes of PC12 cells

To determine the effect of Tau mutants on mitochondrial movement in parallel bundles of MTs, we first used NGF-treated PC12 cells, which have been previously employed for MT-mitochondria studies (Tatebayashi et al., 2004; Morel et al., 2010). We cotransfected Tau constructs and Mito-GFP into PC12 cells and observed the movement of GFP-labeled mitochondria in neurite-like processes 3 d after NGF treatment. Mitochondria were distributed throughout the processes of PC12 cells (left panels of Fig. 4*A*). Mitochondrial motility was recorded over 300 s in randomly selected processes, and examples are shown as kymographs in Figure 4*A*. The number of motile mitochondria was higher in control PC12 cells compared with Tau-overexpressing cells. The percentages of stationary phase of mitochondria, direction of movement, and velocity were quantified (Fig. 4*B–D*). The ratio of stationary phase was 23.0% in control PC12 cells but 47.6% in cells expressing Tau WT and 44.1% for 3A; for 3D, however, the percentage was higher still, 61.3% (Fig. 4*B*). Moving mitochondria in neurites overexpressing Tau 3D were significantly fewer than those in Tau WT or 3A-expressing neurites, indicating the stronger inhibitory activity of Tau 3D. Effect of Tau overexpression on anterograde and retrograde movements is shown in Figure 4*C*. Overexpression of each Tau construct specifically decreased the anterograde movement of mitochondria (compare control with WT/3A/3D in Fig. 4*C*). However, neither Tau 3D nor 3A had further preferential effect on the direction of mitochondrial movement (Fig. 4).

Tau overexpression also affected the velocity of mitochondrial movement in both directions. In control PC12 cells, the velocity was normally distributed with a peak at 0.2–0.3 μm/s (Fig. 4*D*). The mean velocities were around 0.29 ± 0.03 and 0.31 ± 0.04 μm/s for anterograde and retrograde movement, respectively. Tau overexpression shifted the peak to <0.1 μm/s. The percentages of the total anterograde- and retrograde-moving mitochondria moving <0.1 μm/s were 53.3 and 57.7% in Tau WT-expressing PC12 cells, 54.2 and 62.6% in Tau 3A–expressing PC12 cells, and 54.3 and 56.8% in Tau 3D-expressing PC12 cells, respectively. The mean velocities for anterograde and retrograde movement were reduced to 0.19 ± 0.056 and 0.17 ± 0.035 μm/s by Tau WT overexpression, 0.20 ± 0.02 and 0.17 ± 0.07 μm/s by Tau 3A overexpression, and 0.22 ± 0.06 and 0.18 ± 0.04 μm/s by Tau 3D overexpression, respectively. Notably, for Tau 3D there was a second peak of mitochondrial movement with a velocity of ~0.4–0.6 μm/s, particularly in the anterograde direction. Thus, there may be a population of mitochondria that is less affected by Tau 3D. The results that Tau overexpression increased the stationary phase of mitochondria are consistent with previous reports (Trinczek et al., 1999; Thies and Mandelkow, 2007; Stoothoff et al., 2009). Our novel finding was that phosphorylation mimic mutation (3D) at the AT8 Alzheimer sites had an additional effect on mitochondrial motility compared with Tau WT and 3A in neuron-like processes of PC12 cells.

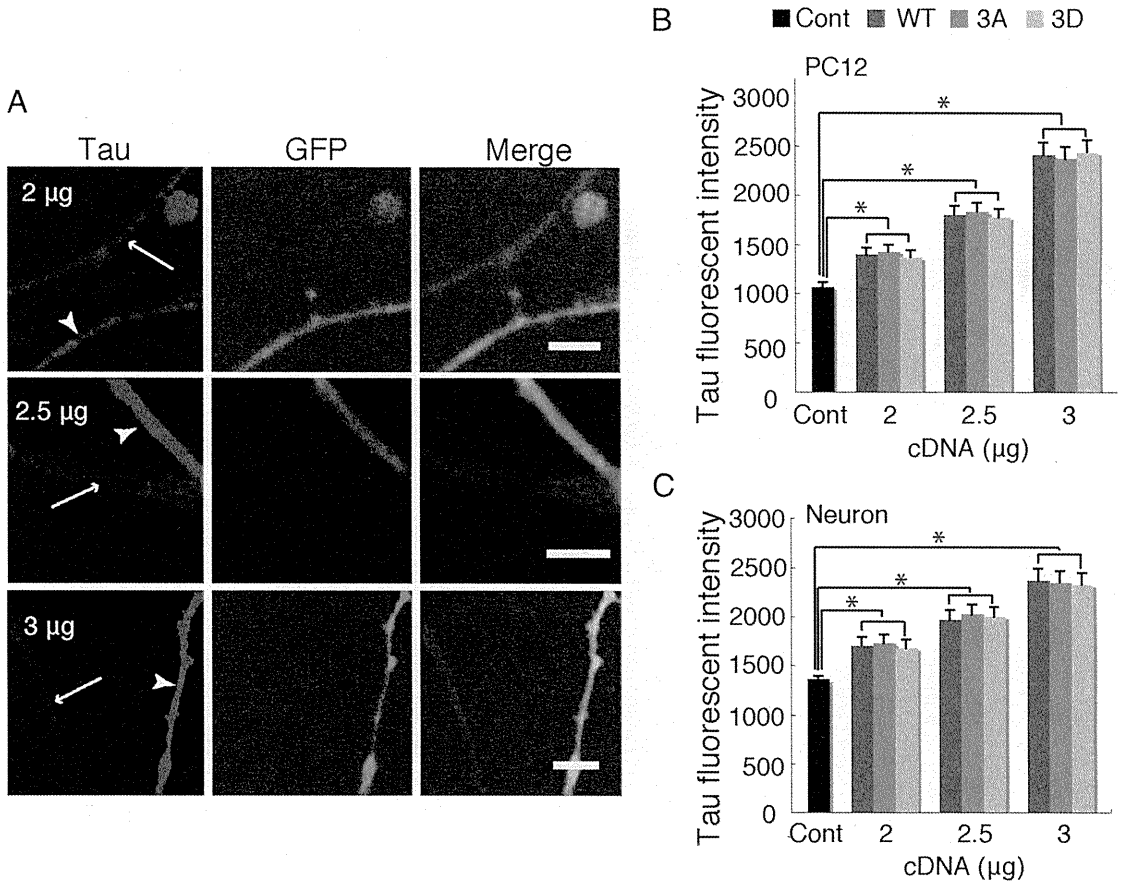

Figure 3. Quantification of levels of Tau overexpression in the PC12 cell neurites and in neuronal axons. ***A***, Immunostaining of cortical neurons overexpressing Tau with anti-human Tau. Plasmids encoding Tau at concentrations of 2, 2.5, and 3 μM were cotransfected with EGFP vector into cultured cortical neurons at DIV6, and these neurons were stained at DIV11. Transfected axons are indicated with arrowheads and un-transfected axons with arrows. Scale bar, 5 μm. ***B***, ***C***, Quantification of Tau expressed in PC12 cell neurites (***B***) and axon of cortical neurons (***C***). ($n = 20$ for each of PC12 cells and neurons, $^*p < 0.01$, one-way ANOVA). Cont, Control.

Increased pausing and decreased velocity of mitochondria in axons of cultured neurons expressing Tau 3D

Tau is predominantly expressed in neuronal axons. We therefore compared the effects of Tau 3D with those of Tau WT or 3A on mitochondrial movement in axons of cultured cortical neurons. Mitochondrial distribution in axons transfected with Tau and Mito-GFP are shown in left panels of Figure 5*A*. During the 300 s observation period, mitochondria exhibited complex motile behavior such as anterograde and retrograde movements with frequent pausing. The duration of stationary phase was 31.6% in control neurons, which was higher than that observed in PC12 cells, consistent with a previous report (Morel et al., 2010). A significant increase in stationary phase was observed after transfection with Tau WT (48.5%) or 3A (46.6%); however, a higher stationary state (64.4%) was caused by Tau 3D (Fig. 5*B*). The stational phase induced by Tau 3D was significantly higher than those induced by Tau WT and 3A, indicating that Tau 3D has stronger inhibitory activity against mitochondrial movement. Direction-dependent inhibition of mitochondrial movement by Tau is summarized in Figure 5C. Tau protein dramatically reduced the population of anterograde-moving mitochondria, consistent with previous reports (Stamer et al., 2002; Dixit et al., 2008; Vershinin et al., 2008; Stoothoff et al., 2009). However, the ratio of mitochondria moving anterogradely and retrogradely was not different among three Tau constructs, indicating that phosphorylation at the AT8 sites does not affect the direction of mitochondrial movements.

Tau overexpression also reduced the velocity of mitochondria in axons. In control neurons, mitochondria showed a peak velocity of 0.2–0.3 μm/s in both directions, and a substantial proportion also moved faster than 0.6 μm/s (Fig. 5*D*). Tau overexpression shifted the peak to a slower rate, with peak velocities of 0.05–0.3 μm/s, depending on the Tau construct. The relative ratio of mitochondria with velocities less than 0.3 μm/s in the anterograde and retrograde directions were 31.0 and 38.2% in control neurons, 88.3 and 84.4% in Tau WT-expressing neurons, 86.9 and 82.6% in Tau 3A-expressing neurons, and 84.7 and 84.4% in Tau 3D-expressing neurons. The mean anterograde and retrograde velocities were 0.55 ± 0.08 and 0.45 ± 0.03 μm/s, respectively, in control cells, but they were reduced to 0.17 ± 0.03 and 0.18 ± 0.06 μm/s in Tau WT-overexpressing neurons, 0.18 ± 0.03 and 0.19 ± 0.07 μm/s in Tau 3A-overexpressing neurons, and 0.18 ± 0.03 and 0.18 ± 0.04 μm/s in Tau 3D-overexpressing neurons. Velocities faster than 1 μm/s, which accounted for 15 and 11% of anterograde and retrograde movements, respectively, in control neurons, were not observed in any Tau-overexpressing neurons. As in PC12 cells, neurons expressing Tau 3D had a small proportion of mitochondria that moved at ~0.5–0.6 μm/s, particularly in the anterograde direction, whereas neurons expressing Tau WT or 3A did not. Thus, Tau with phosphorylation mimic mutation (3D) at the AT8 sites suppressed mitochondrial movement in axons of cultured cortical neurons more than Tau WT or 3A.